SIAM J. SCI. COMPUT.
Vol. 41, No. 3, pp. A1706–A1732

ITERATIVE SOLUTION OF SADDLE-POINT SYSTEMS FROM RADIAL BASIS FUNCTION (RBF) INTERPOLATION*

SABINE LE BORNE† AND MICHAEL WENDE†

Abstract. Scattered data interpolation using conditionally positive definite radial basis functions typically leads to large, dense, and indefinite systems of saddle-point type. Due to ill-conditioning, the iterative solution of these systems requires an effective preconditioner. Using the technique of $\mathcal{H}$-matrices, we propose, analyze, and compare two preconditioning approaches: transformation of the indefinite into a positive definite system using either Lagrangian augmentation or the nullspace method combined with subsequent $\mathcal{H}$-Cholesky preconditioning. Numerical tests support the theoretical condition number estimates and illustrate the performance of the proposed preconditioners which are suitable for problems with up to $N \approx 40000$ centers in two or three spatial dimensions.

Key words. preconditioning, saddle-point systems, radial basis function, scattered data interpolation, hierarchical matrices

AMS subject classifications. 65F08, 65F10, 65D05, 41A05

DOI. 10.1137/18M119063X

1. Introduction.

Scattered data interpolation [27] using radial basis functions (RBFs) requires the solution of a linear system $\boldsymbol{A}\boldsymbol{\alpha} = \boldsymbol{f}$. The matrix $\boldsymbol{A} \in \mathbb{R}^{N\times N}$ contains evaluations of the RBF and is typically dense, large, and ill-conditioned, especially for a high number of scattered data centers N. In the particular case of positive definite RBFs, the matrix $\boldsymbol{A}$ is positive definite which can be exploited in multiple ways for the solution of $\boldsymbol{A}\boldsymbol{\alpha} = \boldsymbol{f}$.

On the other hand, for RBFs which are only conditionally positive definite, the interpolant needs to incorporate a polynomial part which is represented by a matrix $\boldsymbol{B} \in \mathbb{R}^{N\times M}$, where $M \ll N$ (in fact, $M \in \mathcal{O}(1)$) is the dimension of the polynomial space. Now it is necessary to solve a symmetric but indefinite system of saddle-point type,

$$\begin{pmatrix} \boldsymbol{A} & \boldsymbol{B} \\ \boldsymbol{B}^\mathsf{T} & \boldsymbol{O} \end{pmatrix} \begin{pmatrix} \boldsymbol{\alpha} \\ \boldsymbol{\beta} \end{pmatrix} = \begin{pmatrix} \boldsymbol{f} \\ \boldsymbol{0} \end{pmatrix} \quad \Leftrightarrow: \quad \widetilde{\boldsymbol{A}}\widetilde{\boldsymbol{\alpha}} = \widetilde{\boldsymbol{f}}, \tag{1}$$

where $\boldsymbol{O} \in \mathbb{R}^{M\times M}$ is a zero block. Both the indefiniteness of $\widetilde{\boldsymbol{A}}$ and the density of $\boldsymbol{A}$ turn the solution of (1) into a more challenging task compared to the positive definite case. Polynomial or more general functions might also be used to augment the interpolation space in the case of positive definite RBFs, also leading to a saddle point system of the type (1); e.g., in [20], a block diagonal preconditoner in combination with a domain decomposition method is proposed. However, this preconditioner is only applicable when $\boldsymbol{A}$ is positive definite which is no longer the case for only conditionally positive definite RBFs.

In this article we are concerned with the iterative solution of (1) using a preconditioned Krylov subspace method [15, 26, 1, 28]. Our focus is the construction and analysis of preconditioners exploiting the property that $\boldsymbol{A}$ is positive definite on $\ker(\boldsymbol{B}^\mathsf{T})$.

*Submitted to the journal's Methods and Algorithms for Scientific Computing section May 29, 2018; accepted for publication (in revised form) March 18, 2019; published electronically May 21, 2019.

http://www.siam.org/journals/sisc/41-3/M119063.html

†Hamburg University of Technology, 21073 Hamburg, Germany (leborne@tuhh.de, michael.wende@tuhh.de).

1.1. $\mathcal{H}$-matrices. We address the problem of the density of the block $\boldsymbol{A}$ by using the data-sparse technique of hierarchical ($\mathcal{H}$-) matrices [14] which allows the construction of (an approximation to) $\boldsymbol{A}$ using only $\mathcal{O}(N \log N)$ storage and computational time. The multiplication of such an $\mathcal{H}$-matrix $\boldsymbol{A}$ by a vector, which serves as the basic building block of any Krylov subspace method, is of complexity $\mathcal{O}(N \log N)$ as well. Moreover, the explicit representation of $\boldsymbol{A}$ as an $\mathcal{H}$-matrix is the prerequisite for the construction of algebraic preconditioners based on approximate ($\mathcal{H}$-)factorizations such as LU, LDLT, and Cholesky. In interpolation problems with conditionally positive definite RBFs, none of these factorizations are directly applicable since $\boldsymbol{A}$ (as well as diagonal blocks occuring in the factorization process) might be singular. However, we can take advantage of the $\mathcal{H}$-Cholesky factorization after transforming the indefinite system (1) into a positive definite one of about the same size. Based on the representation of $\boldsymbol{A}$ as an $\mathcal{H}$-matrix, we show how the transformation of (1) to positive definite form can be accomplished in $\mathcal{O}(N \log N)$ time using Lagrangian augmentation or the nullspace method. The key observation behind the $\mathcal{O}(N \log N)$ complexity of this transformation process is that both of these methods can be implemented in terms of low-rank updates to $\boldsymbol{A}$. Oftentimes low-rank updates to $\mathcal{H}$-matrices are performed in an approximate sense, but for small M we can perform these updates exactly.

1.2. Lagrangian augmentation. Lagrangian augmentation [13] results in a matrix $\boldsymbol{A}_{\gamma \boldsymbol{W}} := \boldsymbol{A} + \gamma \boldsymbol{B}\boldsymbol{W}\boldsymbol{B}^{\mathsf{T}} \in \mathbb{R}^{N \times N}$, where $\gamma \in \mathbb{R}$, $\boldsymbol{W} \in \mathbb{R}^{M \times M}$ are parameters of the augmentation process. The definition of $\boldsymbol{A}_{\gamma \boldsymbol{W}}$ is initially algebraic, but we show that $\boldsymbol{A}_{\gamma \boldsymbol{W}}$ can be interpreted as the main block of $\widetilde{\boldsymbol{A}}$ using a modification of the original kernel function.

In order to obtain a positive definite $\boldsymbol{A}_{\gamma \boldsymbol{W}}$, it is necessary to choose γ larger than a lower bound depending on the smallest eigenvalue of $\boldsymbol{A}$. For large N, the spectrum of $\boldsymbol{A}$ is unavailable, so for implementation purposes we propose a lower bound depending on the Frobenius norm $\|\boldsymbol{A}\|_{\mathrm{F}}$.

Similar to [13, 4, 10], we derive condition number bounds for the augmented matrix $\boldsymbol{A}_{\gamma \boldsymbol{W}}$. Our results exploit the positive definiteness of $\boldsymbol{A}_{\gamma \boldsymbol{W}}$ which is not assumed in those references. These condition number bounds are put to the test in our numerical experiments.

1.3. Nullspace method. Using the nullspace method [3], we can solve (1) by construction of a basis $\boldsymbol{C}$ of $\ker(\boldsymbol{B}^{\mathsf{T}})$ and projection of $\boldsymbol{A}$ onto $\ker(\boldsymbol{B}^{\mathsf{T}})$. The result is a slightly smaller positive definite system $\boldsymbol{A}' = \boldsymbol{C}^{\mathsf{T}}\boldsymbol{A}\boldsymbol{C} \in \mathbb{R}^{(N-M)\times(N-M)}$.

The construction of $\boldsymbol{C}$ is a sensitive issue because it must be possible to compute $\boldsymbol{A}' = \boldsymbol{C}^{\mathsf{T}}\boldsymbol{A}\boldsymbol{C}$ within the arithmetic of $\mathcal{H}$-matrices and because the condition number of $\boldsymbol{A}'$ depends on the square of the condition number of $\boldsymbol{C}$.

The combination of nullspace methods with $\mathcal{H}$-arithmetic has been exploited in similar contexts before. Nullspace projections using sparse bases have been computed in $\mathcal{H}$-arithmetics in the context of saddle-point problems arising from fluid flow computations in [7]. Regarding RBF interpolation, the use of an orthogonal nullspace basis represented as a sequence of Householder reflectors goes back to [23], and a novelty of our work is to apply this approach to $\mathcal{H}$-matrices. We also found that the interpretation of the nullspace method as an antitriangular factorization [21, 22] of $\widetilde{\boldsymbol{A}}$ is particularly useful for the description and implementation of this method.

An orthogonal nullspace basis is optimal in terms of condition numbers, but we include the construction of sparse nullspace bases as well for comparison purposes. We show bounds on the condition number of $\boldsymbol{C}$ for its construction based on an

LU decomposition with partial pivoting [17, section 9].

1.4. Overview. Our notation for the scattered data interpolation problem is introduced in section 2.

The approximation of $\boldsymbol{A}$ as an $\mathcal{H}$-matrix is sketched in section 3, and more details can be found in [19].

We introduce Lagrangian augmentation to obtain a positive definite main block in section 4 and derive condition number bounds for the augmented main block and its Schur complement.

The nullspace method and its connection to the antitriangular factorization of $\widetilde{\boldsymbol{A}}$ are described in section 5. We compare sparse and orthogonal nullspace bases and analyse the condition numbers of the projected main block.

Numerical results for Lagrangian augmentation and the nullspace method are presented in section 6, and conclusions are summarized in section 7.

2. Scattered data approximation. Scattered data approximation (SDA) refers to the problem of approximating a function $f : \Omega \to \mathbb{R}$ based on evaluations of f at a set of N centers $X = \{\boldsymbol{x}_1, \dots, \boldsymbol{x}_N\}$ in a bounded domain $\Omega \subseteq \mathbb{R}^d$. In principle, the spatial dimension $d \in \mathbb{N}$ is arbitrary but here assumed to be small and fixed, i.e., $d \in \{2, 3\}$. The set X is scattered in the sense that there is no restriction on the precise locations of centers.

Using a hybrid interpolation scheme based on both RBFs and polynomials, the SDA problem is approached by finding an interpolant $s : \Omega \to \mathbb{R}$ coinciding with f at X. Here the interpolant s is constructed in terms of a radial kernel

$$\Phi : \mathbb{R}^d \times \mathbb{R}^d \to \mathbb{R}, \quad \Phi(\boldsymbol{x}, \boldsymbol{y}) := \phi(\|\boldsymbol{x} - \boldsymbol{y}\|_2),$$

where $\phi : \mathbb{R} \to \mathbb{R}$ is an RBF and $\|\cdot\|_2$ denotes the Euclidean norm. The hybrid RBF interpolant s also relies on the space π_m^d of d-variate polynomials of degree less than $m \in \mathbb{N}_0$,

$$\pi_m^d := \left\{ p(\boldsymbol{x}) = \sum_{\|\boldsymbol{n}\|_1 < m} \beta_{\boldsymbol{n}} \boldsymbol{x}^{\boldsymbol{n}} \;\middle|\; \boldsymbol{n} \in \mathbb{N}_0^d,\ \beta_{\boldsymbol{n}} \in \mathbb{R} \right\}. \tag{2}$$

Here, for a multiindex $\boldsymbol{n} \in \mathbb{N}_0^d$ and a point $\boldsymbol{x} \in \mathbb{R}^d$, we use the notation

$$\|\boldsymbol{n}\|_1 := \sum_{i=1}^d n_i, \quad \boldsymbol{x}^{\boldsymbol{n}} := \prod_{i=1}^d x_i^{n_i}.$$

The dimension of the polynomial space is $M := \dim(\pi_m^d) = \binom{m+d-1}{d}$ with $m = 0$ corresponding to the trivial space $\pi_0^d = \{0\}$. We always assume that m and, therefore, M are small and fixed compared to N.

Choosing a basis $p_1, \dots, p_M$ of π_m^d, the interpolant s is written as

$$s(\boldsymbol{x}) = \sum_{j=1}^N \alpha_j \Phi(\boldsymbol{x}_j, \boldsymbol{x}) + \sum_{j=1}^M \beta_j p_j(\boldsymbol{x}) \tag{3}$$

with RBF coefficients $\alpha_1, \dots, \alpha_N \in \mathbb{R}$ and polynomial coefficients $\beta_1, \dots, \beta_M \in \mathbb{R}$. These coefficients are determined by the interpolation conditions

$$s|_X = f|_X \quad \Leftrightarrow: \quad s(\boldsymbol{x}_i) = f(\boldsymbol{x}_i), \quad i = 1, \dots, N, \tag{4}$$

together with a restriction on the RBF coefficients in the form

$$\sum_{j=1}^{N} \alpha_j p_i(\boldsymbol{x}_j) = 0, \quad i = 1, \dots, M. \tag{5}$$

Combining (4) and (5) results in $N+M$ linear equations to which we refer as extended interpolation equations. These can be written in matrix form (1), where

$$\boldsymbol{A} = \big(\Phi(\boldsymbol{x}_i, \boldsymbol{x}_j)\big) \in \mathbb{R}^{N\times N}, \quad \boldsymbol{B} = \big(p_j(\boldsymbol{x}_i)\big) \in \mathbb{R}^{N\times M},$$
$$\boldsymbol{f} = \big(f(\boldsymbol{x}_i)\big) \in \mathbb{R}^{N}, \quad \boldsymbol{\alpha} = (\alpha_i) \in \mathbb{R}^{N}, \quad \boldsymbol{\beta} = (\beta_i) \in \mathbb{R}^{M}.$$

The main block $\boldsymbol{A}$ of the extended interpolation matrix $\widetilde{\boldsymbol{A}}$ is symmetric due to the symmetry of the radial kernel Φ. The polynomial block $\boldsymbol{B}$ is assumed to have full rank M which is equivalent to the requirement that X is unisolvent with respect to π_m^d. The unisolvent property of X means that $p = 0$ is the only polynomial $p \in \pi_m^d$ vanishing on X [27, Definition 2.6].

For the class of conditionally positive definite RBFs [27, section 8], the main block $\boldsymbol{A}$ is positive definite on the nullspace of $\boldsymbol{B}^{\mathsf{T}}$ provided that m is chosen large enough. The smallest $m_0 \in \mathbb{N}_0$ achieving this property is called the order of the RBF ϕ [27, Theorem 8.3], and a positive definite RBF is conditionally positive definite of order $m_0 = 0$.

THEOREM 1. *Let $X = \{\boldsymbol{x}_1, \dots, \boldsymbol{x}_N\}$ be a set of N pairwise distinct centers. Assume that ϕ is conditionally positive definite of order m_0, and let $m \geq m_0$. Then $\boldsymbol{A}$ is positive definite on $\ker(\boldsymbol{B}^{\mathsf{T}})$, i.e., $\boldsymbol{\alpha}^{\mathsf{T}}\boldsymbol{A}\boldsymbol{\alpha} > 0$ for all $\boldsymbol{\alpha} \in \ker(\boldsymbol{B}^{\mathsf{T}}) \setminus \{\boldsymbol{0}\}$.*

The positive definiteness of $\boldsymbol{A}$ on $\ker(\boldsymbol{B}^{\mathsf{T}})$, combined with the full-rank assumption on $\boldsymbol{B}$, implies the invertibility of the saddle-point matrix $\widetilde{\boldsymbol{A}}$. We will make frequent use of Theorem 1 in the discussion of the solution techniques in the following sections.

3. Hierarchical matrices. We can approximate the main block $\boldsymbol{A}$ of the saddle-point matrix $\widetilde{\boldsymbol{A}}$ as a hierarchical ($\mathcal{H}$-) matrix with almost optimal storage complexity $\mathcal{O}(N \log N)$ since the RBFs considered here are asymptotically smooth [14, Definition 4.14], [19].

Since the polynomial degree m is small, the offdiagonal block $\boldsymbol{B}$ of $\widetilde{\boldsymbol{A}}$ can be represented as a full matrix in $\mathcal{O}(N)$ storage, leading to an $\mathcal{H}$-matrix $\widetilde{\boldsymbol{A}}$.

The $\mathcal{H}$-matrix construction of $\boldsymbol{A}$ might be based on a separable expansion

$$\Phi(\boldsymbol{x}, \boldsymbol{y}) = \sum_{n=1}^{\infty} u_n(\boldsymbol{x}) \cdot v_n(\boldsymbol{y}). \tag{6}$$

An approximation of $\Phi(\boldsymbol{x}, \boldsymbol{y})$ is obtained by truncating (6) after a number of k leading terms, referred to as the representation rank.

Separable expansions targeting specific RBFs can be derived analytically, e.g., for the class of generalized multiquadric RBFs as in [11, 25]. Analytic expansions applicable to a wider class of RBFs include polynomial interpolation at Chebyshev nodes on a tensor grid and Taylor expansion [14, section 4.3].

We use the algebraic procedure by the name of adaptive cross approximation (ACA) [14, section 9.4] where the desired approximation accuracy can be specified in terms of a threshold parameter $\epsilon_{\mathrm{ACA}} > 0$.

For a given approximation accuracy, the amount of memory required for the main block $\boldsymbol{A}$ using the ACA approach is typically much lower compared to analytic expansion alternatives [19].

Low-rank approximations obtained from truncating a separable expansion are only applicable to certain blocks of the entire $\boldsymbol{A}$, whereas other blocks have to be stored as full matrices. The efficiency of this approximation scheme relies on the fact that full blocks are small and that the number of full blocks is limited. An illustration of the block structures obtained from approximating $\boldsymbol{A}$ as an $\mathcal{H}$-matrix in $d = 1, 2, 3$ dimensions is shown in Figure 1.

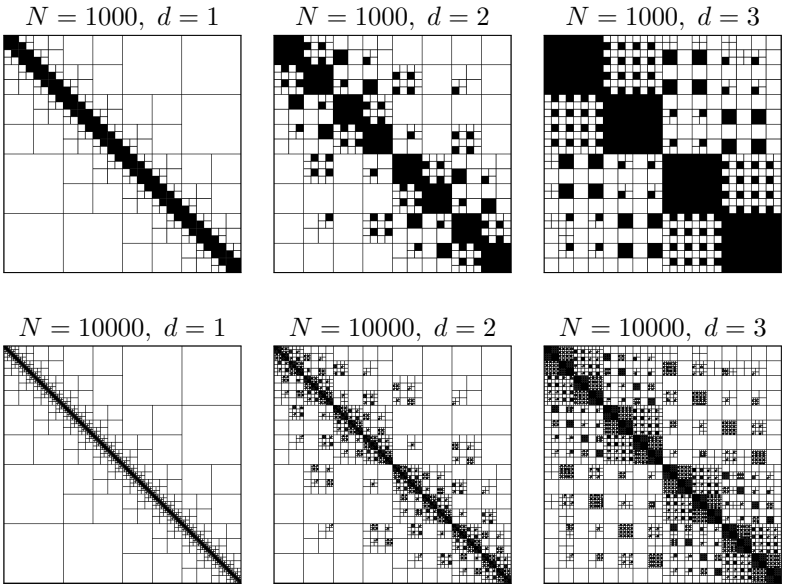

FIG. 1. *Illustration of the block structures obtained from setting up the main block* $\boldsymbol{A}$ *of the extended interpolation matrix* $\widetilde{\boldsymbol{A}}$ *using* $N = 1000$ *and* $N = 10000$ *Halton centers in unit cubes in* $d = 1, 2, 3$ *dimensions.*

3.1. Algebraic preconditioning. The framework of $\mathcal{H}$-matrices supports the computation of approximate Cholesky, LU, and LDLT decompositions with complexity $\mathcal{O}(N(\log N)^2)$ in terms of both time and memory [14, section 7.6].

In principle, these factorizations can be performed very accurately such that the corresponding linear system can be solved directly using block triangular and diagonal solves. A disadvantage of this approach is that it requires a high accuracy which leads to a rather expensive factorization process. When used as preconditioners within an iterative solver, it often suffices to compute these factorizations with comparatively low accuracy.

In the context of RBF interpolation, the simplest case occurs using a positive definite RBF without polynomials since the main block can be subjected to an $\mathcal{H}$-Cholesky factorization [14, section 7.6.4].

When the interpolant is set up using a positive definite RBF together with a possibly nonempty polynomial part, we can still compute the $\mathcal{H}$-LU decomposition [14, section 7.6.4] of the extended interpolation matrix.

None of these $\mathcal{H}$-factorizations are directly applicable to the extended interpolation matrix when conditionally positive definite RBFs are considered because the

fixed block structure of $\mathcal{H}$-matrices disallows pivoting during the factorization process. Without pivoting, the existence of these factorizations requires that every leading principal minor of $\boldsymbol{A}$ is regular. In the example of thin plate splines (56), the entire diagonal of $\widetilde{\boldsymbol{A}}$ is zero such that any factorization will break down at the first step.

We propose using Lagrangian augmentation or the nullspace method to avoid these issues since they turn the system into a positive definite one which we then solve iteratively using an $\mathcal{H}$-Cholesky preconditioner. Further types of preconditioners for positive definite systems as well as inner iterative solvers for the resulting subproblems remain a subject of future study.

4. Lagrangian augmentation. Lagrangian augmentation [13, 4] is a preconditioning technique for saddle-point systems where the main block $\boldsymbol{A}$ of the saddle-point matrix $\widetilde{\boldsymbol{A}}$ is modified in order to aid the subsequent solution process. In general, Lagrangian augmentation by itself does not lead to an effective preconditioner which can be used for the original system directly. Instead, Lagrangian augmentation is used as a preprocessing step such that another type of preconditioner, which would have been unavailable or less effective for the original system, may be constructed for the modified system. Although Lagrangian augmentation methods are applicable to both symmetric and unsymmetric saddle-point matrices, we will restrict our discussion to a symmetric saddle-point matrix $\widetilde{\boldsymbol{A}}$ as in (1).

The Lagrangian augmentation approach can be viewed as a special kind of regularization [12, Chapter 1] which does not change the solution of (1). To this end we, assume that (1) is the Karush–Kuhn–Tucker (KKT) system associated with the constrained minimization problem [9, section 5.5.3]

$$\min_{\boldsymbol{\alpha}} \quad \frac{1}{2}\boldsymbol{\alpha}^{\mathsf{T}}\boldsymbol{A}\boldsymbol{\alpha} - \boldsymbol{\alpha}^{\mathsf{T}}\boldsymbol{f} \quad \text{s.t.} \quad \boldsymbol{B}^{\mathsf{T}}\boldsymbol{\alpha} = \boldsymbol{0}. \tag{7}$$

Then the RBF coefficients $\boldsymbol{\alpha}$ correspond to the unique solution of (7), and the polynomial coefficients $\boldsymbol{\beta}$ are the associated Lagrange multipliers. Using a positive semidefinite matrix $\boldsymbol{M}$, problem (7) can be regularized by adding a positive multiple of $\boldsymbol{\alpha}^{\mathsf{T}}\boldsymbol{M}\boldsymbol{\alpha}$ to the objective function to impose a penalty on the size of the RBF coefficients $\boldsymbol{\alpha}$. Then the regularized problem reads

$$\min_{\boldsymbol{\alpha}} \quad \frac{1}{2}\boldsymbol{\alpha}^{\mathsf{T}}\boldsymbol{A}\boldsymbol{\alpha} + \frac{\gamma}{2}\boldsymbol{\alpha}^{\mathsf{T}}\boldsymbol{M}\boldsymbol{\alpha} - \boldsymbol{\alpha}^{\mathsf{T}}\boldsymbol{f} \quad \text{s.t.} \quad \boldsymbol{B}^{\mathsf{T}}\boldsymbol{\alpha} = \boldsymbol{0}, \tag{8}$$

where the parameter $\gamma \geq 0$ is used to control the penalty term. Since $\boldsymbol{A}$ is positive definite on $\ker(\boldsymbol{B}^{\mathsf{T}})$, it follows that the regularized problem always has a unique solution as well. The KKT system corresponding to (8) is

$$\begin{pmatrix} \boldsymbol{A} + \gamma\boldsymbol{M} & \boldsymbol{B} \\ \boldsymbol{B}^{\mathsf{T}} & \boldsymbol{O} \end{pmatrix} \begin{pmatrix} \boldsymbol{\alpha} \\ \boldsymbol{\beta} \end{pmatrix} = \begin{pmatrix} \boldsymbol{f} \\ \boldsymbol{0} \end{pmatrix}, \tag{9}$$

where the modified main block $\boldsymbol{A} + \gamma\boldsymbol{M}$ is again positive definite on $\ker(\boldsymbol{B})^{\mathsf{T}}$. The solution of (7) coincides with the solution of (8) if the penalty $\boldsymbol{\alpha}^{\mathsf{T}}\boldsymbol{M}\boldsymbol{\alpha}$ is zero for all $\boldsymbol{\alpha} \in \ker(\boldsymbol{B})^{\mathsf{T}}$, and such a penalty is of the form $\boldsymbol{M} = \boldsymbol{B}\boldsymbol{W}\boldsymbol{B}^{\mathsf{T}}$ for some positive definite matrix $\boldsymbol{W} \in \mathbb{R}^{M\times M}$. In this case the modified system (9) is of the form

$$\begin{pmatrix} \boldsymbol{A} + \gamma\boldsymbol{B}\boldsymbol{W}\boldsymbol{B}^{\mathsf{T}} & \boldsymbol{B} \\ \boldsymbol{B}^{\mathsf{T}} & \boldsymbol{O} \end{pmatrix} \begin{pmatrix} \boldsymbol{\alpha} \\ \boldsymbol{\beta} \end{pmatrix} = \begin{pmatrix} \boldsymbol{f} \\ \boldsymbol{0} \end{pmatrix} \quad \Leftrightarrow: \quad \widetilde{\boldsymbol{A}}_{\gamma\boldsymbol{W}}\widetilde{\boldsymbol{\alpha}} = \widetilde{\boldsymbol{f}}, \tag{10}$$

where $\widetilde{\boldsymbol{A}}_{\gamma\boldsymbol{W}}$ denotes the augmented system matrix. The augmented main block $\boldsymbol{A}_{\gamma\boldsymbol{W}} := \boldsymbol{A} + \gamma\boldsymbol{B}\boldsymbol{W}\boldsymbol{B}^{\mathsf{T}}$ can be computed as a low-rank update to the original main

block $\boldsymbol{A}$ within the arithmetics of $\mathcal{H}$-matrices. This was done in [6] where Lagrangian augmentation was applied to a nonsymmetric saddle-point matrix arising from the discretization of the Navier–Stokes equations in two and three dimensions. Different from our application, the matrices $\boldsymbol{A}$ and $\boldsymbol{B}$ in [6] are sparse. Since in [6] not only $\boldsymbol{A}$ but also $\boldsymbol{B}$ is an $\mathcal{H}$-matrix and has a large number of $\mathcal{O}(N)$ columns, operations involving $\boldsymbol{B}$ cannot be performed in exact arithmetic. In our case, $\boldsymbol{A}_{\gamma\boldsymbol{W}}$ can be computed without any truncation since the dimension of the polynomial space M is small.

The augmented system (10) can also be obtained from the original system (1) by multiplication from the left with a triangular block preconditioner of the form

$$\widetilde{\boldsymbol{N}}_{\gamma\boldsymbol{W}} = \begin{pmatrix} \boldsymbol{I}_N & \gamma\boldsymbol{B}\boldsymbol{W} \\ \boldsymbol{O} & \boldsymbol{I}_M \end{pmatrix}, \quad \text{with} \quad \widetilde{\boldsymbol{N}}_{\gamma\boldsymbol{W}}^{-1} = \widetilde{\boldsymbol{N}}_{-\gamma\boldsymbol{W}}. \tag{11}$$

This corresponds to adding a multiple of the second block row to the first in (1) where the symmetry of $\widetilde{\boldsymbol{A}}$ and the special form of the right-hand side $\widetilde{\boldsymbol{f}}$ are preserved because of the presence of zero blocks. The left-sided preconditioning of $\widetilde{\boldsymbol{A}}$ can also be viewed as a two-sided preconditioning since

$$\widetilde{\boldsymbol{A}}_{\gamma\boldsymbol{W}} = \widetilde{\boldsymbol{N}}_{\gamma\boldsymbol{W}}\widetilde{\boldsymbol{A}} = \widetilde{\boldsymbol{N}}_{\frac{\gamma}{2}\boldsymbol{W}}\widetilde{\boldsymbol{A}}\widetilde{\boldsymbol{N}}_{\frac{\gamma}{2}\boldsymbol{W}}^{\mathsf{T}}.$$

4.1. Analytical interpretation. Up to now we have described Lagrangian augmentation from a purely algebraic perspective. Alternatively, the augmented main block $\boldsymbol{A}_{\gamma\boldsymbol{W}}$ can be obtained by using a modified kernel function Φ^{aug} defined in terms of Φ and an alternate basis $p_1^{\text{aug}}, \dots, p_M^{\text{aug}}$ for the polynomial space π_m^d as

$$\Phi^{\text{aug}}(\boldsymbol{x}, \boldsymbol{y}) = \Phi(\boldsymbol{x}, \boldsymbol{y}) + \sum_{j=1}^{M} p_j^{\text{aug}}(\boldsymbol{x})\, p_j^{\text{aug}}(\boldsymbol{y}). \tag{12}$$

Note that Φ^{aug} is conditionally positive definite of the same order as Φ. If we define $\boldsymbol{A}^{\text{aug}} \in \mathbb{R}^{N\times N}$ via $\boldsymbol{A}^{\text{aug}}_{i,j} = \Phi^{\text{aug}}(\boldsymbol{x}_i, \boldsymbol{x}_j)$, we can choose $p_1^{\text{aug}}, \dots, p_M^{\text{aug}}$ such that $\boldsymbol{A}^{\text{aug}} = \boldsymbol{A}_{\gamma\boldsymbol{W}}$. The choice of $p_1^{\text{aug}}, \dots, p_M^{\text{aug}}$ is not unique but one possibility is to use a Cholesky decomposition $\gamma\boldsymbol{W} = \boldsymbol{L}\boldsymbol{L}^{\mathsf{T}}$ and set

$$p_j^{\text{aug}} = \sum_{i=j}^{M} L_{i,j} p_i, \quad j = 1, \dots, M.$$

Then using $\boldsymbol{B}^{\text{aug}} \in \mathbb{R}^{N\times M}$ with $B^{\text{aug}}_{i,j} = p_j^{\text{aug}}(\boldsymbol{x}_i)$, the augmented main block becomes

$$\boldsymbol{A}_{\gamma\boldsymbol{W}} = \boldsymbol{A} + \gamma\boldsymbol{B}\boldsymbol{W}\boldsymbol{B}^{\mathsf{T}} = \boldsymbol{A} + \boldsymbol{B}\boldsymbol{L}\boldsymbol{L}^{\mathsf{T}}\boldsymbol{B}^{\mathsf{T}} = \boldsymbol{A} + \boldsymbol{B}^{\text{aug}}(\boldsymbol{B}^{\text{aug}})^{\mathsf{T}} = \boldsymbol{A}^{\text{aug}}.$$

To the best of our knowledge, the connection between the augmented kernel Φ^{aug} and the algebraic process of Lagrangian augmentation has not appeared elsewhere. However, the construction of Φ^{aug} is similar to the definition of the positive definite kernel K in [27, section 12.3] which is defined in terms of a set $\Xi = \{\boldsymbol{\xi}_1, \dots, \boldsymbol{\xi}_M\} \subset \mathbb{R}^d$ of M unisolvent centers for π_m^d. Assume that $p_1, \dots, p_M$ form a Lagrange basis of π_m^d with respect to the set Ξ, i.e.,

$$p_i(\boldsymbol{x}_j) = \delta_{i,j}, \quad i, j = 1, \dots, M,$$

where $\delta_{i,j}$ is the Kronecker operator. Using the conditionally positive definite kernel [27, eq. (12.4)]

$$\kappa(\boldsymbol{x},\boldsymbol{y}) := \Phi(\boldsymbol{x},\boldsymbol{y}) - \sum_{i=1}^{M} p_i(\boldsymbol{x})\ \Phi(\boldsymbol{\xi}_i,\boldsymbol{y}) - \sum_{j=1}^{M} p_j(\boldsymbol{y})\ \Phi(\boldsymbol{x},\boldsymbol{\xi}_j) + \sum_{i=1}^{M}\sum_{j=1}^{M} p_i(\boldsymbol{x})\ p_j(\boldsymbol{y})\ \Phi(\boldsymbol{\xi}_i,\boldsymbol{\xi}_j),$$

the positive definite kernel K is defined as

$$K(\boldsymbol{x},\boldsymbol{y}) = \kappa(\boldsymbol{x},\boldsymbol{y}) + \sum_{j=1}^{M} p_j(\boldsymbol{x}) p_j(\boldsymbol{y}) \tag{13}$$

with the sum in (13) resembling the sum in (12). Note that the definition of the positive definite kernel K does not depend on X. On the other hand, Φ^{aug} will usually depend on X when γ and $\boldsymbol{W}$ are chosen algebraically in terms of $\boldsymbol{A}$ and $\boldsymbol{B}$ as suggested by Theorem 2 below.

4.2. Positive definiteness. Our primary motivation for studying Lagrangian augmentation is that, for γ large enough, we obtain a positive definite main block $\boldsymbol{A}_{\gamma\boldsymbol{W}}$. In the following, $\sigma_{\min}(\boldsymbol{A})$ and $\sigma_{\max}(\boldsymbol{A})$ denote the smallest and largest singular values of any matrix $\boldsymbol{A}$, respectively. Similarly $\lambda_{\min}(\boldsymbol{A})$ and $\lambda_{\max}(\boldsymbol{A})$ are used for the extremal eigenvalues of $\boldsymbol{A}$.

THEOREM 2. *Assume that the extended interpolation matrix $\widetilde{\boldsymbol{A}}$ has been set up such that the columns of $\boldsymbol{B}$ are linearly independent and $\boldsymbol{A}$ is positive definite on* $\ker(\boldsymbol{B}^{\mathsf{T}})$. *Then the augmented main block $\boldsymbol{A}_{\gamma\boldsymbol{W}} = \boldsymbol{A} + \gamma\boldsymbol{B}\boldsymbol{W}\boldsymbol{B}^{\mathsf{T}}$ is positive definite if*

$$\gamma > \frac{|\lambda_{\min}(\boldsymbol{A})|}{\sigma_{\min}(\boldsymbol{B}\boldsymbol{W}^{1/2})^2}. \tag{14}$$

Proof. Let $\boldsymbol{U} = (\boldsymbol{U}_1, \boldsymbol{U}_2) \in \mathbb{R}^{N\times N}$ be an orthonormal matrix with columns of $\boldsymbol{U}_1$ given by eigenvectors for positive eigenvalues of $\boldsymbol{A}$. It follows that $\boldsymbol{U}_1^{\mathsf{T}}\boldsymbol{A}\boldsymbol{U}_2 = \boldsymbol{O}$. In particular, it holds that

$$\ker(\boldsymbol{B}^{\mathsf{T}}) \subseteq \mathrm{im}(\boldsymbol{U}_1) = \{\boldsymbol{x}\in\mathbb{R}^N \mid \boldsymbol{x}^{\mathsf{T}}\boldsymbol{A}\boldsymbol{x} > 0\} \cup \{\boldsymbol{0}\}. \tag{15}$$

Due to the orthonormality of $\boldsymbol{U}$, for any $\boldsymbol{x}\in\mathbb{R}^N$ there exists a $\boldsymbol{y}\in\mathbb{R}^N$ such that

$$\boldsymbol{x} = \boldsymbol{U}\boldsymbol{y} = \boldsymbol{U}_1\boldsymbol{y}_1 + \boldsymbol{U}_2\boldsymbol{y}_2, \quad \|\boldsymbol{x}\|_2^2 = \|\boldsymbol{y}\|_2^2 = \|\boldsymbol{y}_1\|_2^2 + \|\boldsymbol{y}_2\|_2^2, \quad \boldsymbol{y}_i = \boldsymbol{U}_i^{\mathsf{T}}\boldsymbol{x}, \quad i = 1,2. \tag{16}$$

We choose another orthonormal matrix $\boldsymbol{V} = (\boldsymbol{V}_1, \boldsymbol{V}_2)$ such that $\mathrm{im}(\boldsymbol{V}_1) = \ker(\boldsymbol{B}^{\mathsf{T}})$ and $\mathrm{im}(\boldsymbol{V}_2) = \mathrm{im}(\boldsymbol{B})$. The positive definiteness of $\boldsymbol{A}$ on $\mathrm{im}(\boldsymbol{V}_1)$ implies $\mathrm{im}(\boldsymbol{V}_1) \subseteq \mathrm{im}(\boldsymbol{U}_1)$. Based on $\boldsymbol{V}$, we use a second representation of $\boldsymbol{x}$ as

$$\boldsymbol{x} = \boldsymbol{V}\boldsymbol{z} = \boldsymbol{V}_1\boldsymbol{z}_1 + \boldsymbol{V}_2\boldsymbol{z}_2, \quad \|\boldsymbol{x}\|_2^2 = \|\boldsymbol{z}\|_2^2 = \|\boldsymbol{z}_1\|_2^2 + \|\boldsymbol{z}_2\|_2^2, \quad \boldsymbol{z}_i = \boldsymbol{V}_i^{\mathsf{T}}\boldsymbol{x}, \quad i = 1,2. \tag{17}$$

Now $\mathrm{im}(\boldsymbol{V}_{,i}\,1) \subseteq \mathrm{im}(\boldsymbol{U}_1)$ implies

$$\|\underbrace{\boldsymbol{V}_1^{\mathsf{T}}\boldsymbol{x}}_{\boldsymbol{z}_1}\|_2 \le \|\underbrace{\boldsymbol{U}_1^{\mathsf{T}}\boldsymbol{x}}_{\boldsymbol{y}_1}\|_2, \quad \text{i.e.,} \quad \|\boldsymbol{z}_2\|_2^2 \ge \|\boldsymbol{y}_2\|_2^2. \tag{18}$$

It follows that

$$\begin{aligned}(19)\quad \boldsymbol{x}^\mathsf{T}\left(\boldsymbol{A}+\gamma\boldsymbol{B}\boldsymbol{W}\boldsymbol{B}^\mathsf{T}\right)\boldsymbol{x} &= \boldsymbol{y}_1^\mathsf{T}\boldsymbol{U}_1^\mathsf{T}\boldsymbol{A}\boldsymbol{U}_1\boldsymbol{y}_1+\boldsymbol{y}_2^\mathsf{T}\boldsymbol{U}_2^\mathsf{T}\boldsymbol{A}\boldsymbol{U}_2\boldsymbol{y}_2+\gamma\,\boldsymbol{z}_2^\mathsf{T}\boldsymbol{V}_2^\mathsf{T}\boldsymbol{B}\boldsymbol{W}\boldsymbol{B}^\mathsf{T}\boldsymbol{V}_2\boldsymbol{z}_2\\ &\geq \boldsymbol{y}_1^\mathsf{T}\boldsymbol{U}_1^\mathsf{T}\boldsymbol{A}\boldsymbol{U}_1\boldsymbol{y}_1-\sigma_{\max}\left(\boldsymbol{U}_2^\mathsf{T}\boldsymbol{A}\boldsymbol{U}_2\right)\|\boldsymbol{y}_2\|_2^2+\gamma\,\sigma_{\min}(\boldsymbol{B}\boldsymbol{W}^{1/2})^2\,\|\boldsymbol{z}_2\|_2^2\\ &\geq \boldsymbol{y}_1^\mathsf{T}\boldsymbol{U}_1^\mathsf{T}\boldsymbol{A}\boldsymbol{U}_1\boldsymbol{y}_1+\left(\gamma\,\sigma_{\min}(\boldsymbol{B}\boldsymbol{W}^{1/2})^2-\sigma_{\max}\left(\boldsymbol{U}_2^\mathsf{T}\boldsymbol{A}\boldsymbol{U}_2\right)\right)\,\|\boldsymbol{z}_2\|_2^2,\end{aligned}$$

where we used $\boldsymbol{B}^\mathsf{T}\boldsymbol{V}_1=\boldsymbol{O}$ and $\boldsymbol{U}_1^\mathsf{T}\boldsymbol{A}\boldsymbol{U}_2=\boldsymbol{O}$ in the first line and then applied the inequality in (18). Within the last line of (19), we have $\lambda_{\min}(\boldsymbol{A})=-\sigma_{\max}(\boldsymbol{U}_2^\mathsf{T}\boldsymbol{A}\boldsymbol{U}_2)$ since $\mathrm{im}(\boldsymbol{U}_2)=\{\boldsymbol{x}\in\mathbb{R}^N\mid \boldsymbol{x}^\mathsf{T}\boldsymbol{A}\boldsymbol{x}\leq 0\}$. Then the last expression in (19) is positive if

$$\gamma\,\sigma_{\min}(\boldsymbol{B}\boldsymbol{W}^{1/2})^2-\sigma_{\max}\left(\boldsymbol{U}_2^\mathsf{T}\boldsymbol{A}\boldsymbol{U}_2\right)>0\quad\Leftrightarrow\quad\gamma>\frac{|\lambda_{\min}(\boldsymbol{A})|}{\sigma_{\min}(\boldsymbol{B}\boldsymbol{W}^{1/2})^2}$$

since $\boldsymbol{x}\neq\boldsymbol{0}$ implies that $\boldsymbol{y}_1\neq\boldsymbol{0}$ or $\boldsymbol{z}_2\neq\boldsymbol{0}$. The latter implication holds because

$$\boldsymbol{x}\neq\boldsymbol{0}\quad\Rightarrow\quad\boldsymbol{y}\neq\boldsymbol{0}\quad\Rightarrow\quad\boldsymbol{y}_1\neq\boldsymbol{0}\vee\boldsymbol{y}_2\neq\boldsymbol{0}\quad\overset{(18)}{\Rightarrow}\quad\boldsymbol{y}_1\neq\boldsymbol{0}\vee\boldsymbol{z}_2\neq\boldsymbol{0}$$

where we used $\boldsymbol{y}_2\neq\boldsymbol{0}\Rightarrow\boldsymbol{z}_2\neq\boldsymbol{0}$ as a consequence of (18). ∎

Remark 3. If the augmented main block $\boldsymbol{A}_{\gamma\boldsymbol{W}}$ is positive definite, then the Schur complement $\boldsymbol{S}_{\gamma\boldsymbol{W}}=-\boldsymbol{B}^\mathsf{T}\boldsymbol{A}_{\gamma\boldsymbol{W}}^{-1}\boldsymbol{B}$ is negative definite.

After Lagrangian augmentation, blockwise Gaussian elimination transforms system (10) to block-triangular form

$$(20)\qquad\begin{pmatrix}\boldsymbol{A}_{\gamma\boldsymbol{W}} & \boldsymbol{B}\\ \boldsymbol{O} & \boldsymbol{S}_{\gamma\boldsymbol{W}}\end{pmatrix}\begin{pmatrix}\boldsymbol{\alpha}\\ \boldsymbol{\beta}\end{pmatrix}=\begin{pmatrix}\boldsymbol{f}\\ -\boldsymbol{B}^\mathsf{T}\boldsymbol{A}_{\gamma\boldsymbol{W}}^{-1}\boldsymbol{f}\end{pmatrix}.$$

Based on (20), we can use back-substitution to compute $\boldsymbol{\alpha}$ and $\boldsymbol{\beta}$ as

$$(21a)\qquad\boldsymbol{\beta}=-\boldsymbol{S}_{\gamma\boldsymbol{W}}^{-1}\left(\boldsymbol{B}^\mathsf{T}\boldsymbol{A}_{\gamma\boldsymbol{W}}^{-1}\right)\boldsymbol{f},$$

$$(21b)\qquad\boldsymbol{\alpha}=\boldsymbol{A}_{\gamma\boldsymbol{W}}^{-1}\left(\boldsymbol{f}-\boldsymbol{B}\boldsymbol{\beta}\right).$$

An (approximate) solution for first $\boldsymbol{\beta}$ and then $\boldsymbol{\alpha}$ is obtained as follows: Replace $\boldsymbol{A}_{\gamma\boldsymbol{W}}$ by an $\mathcal{H}$-matrix $\boldsymbol{A}_{\gamma\boldsymbol{W}}^{\mathcal{H}}$, compute the dense matrix $\boldsymbol{B}^\mathsf{T}(\boldsymbol{A}_{\gamma\boldsymbol{W}}^{\mathcal{H}})^{-1}$ to high accuracy through some inner iterative method using, e.g., $\mathcal{H}$-Cholesky preconditioning, and use it in (21a) as well as to compute the (small) Schur complement $\boldsymbol{S}_{\gamma\boldsymbol{W}}=-(\boldsymbol{B}^\mathsf{T}(\boldsymbol{A}_{\gamma\boldsymbol{W}}^{\mathcal{H}})^{-1})\boldsymbol{B}$ as a dense matrix. Another linear system involving $\boldsymbol{A}_{\gamma\boldsymbol{W}}^{\mathcal{H}}$ appears in (21b) which again can be solved iteratively using the conjugate gradient (CG) algorithm with $\mathcal{H}$-Cholesky preconditioning. The inverse of $\boldsymbol{S}_{\gamma\boldsymbol{W}}$ in (21a) can be computed directly, e.g., via Cholesky decomposition of $-\boldsymbol{S}_{\gamma\boldsymbol{W}}$, since this matrix is small.

As an alternative to the solution of (20) and pursued in our numerical experiments, one can apply the GMRES algorithm directly to (10) using an $\mathcal{H}$-LU preconditioner. Preconditioning of $\widetilde{\boldsymbol{A}}_{\gamma\boldsymbol{W}}$ using an $\mathcal{H}$-LU decomposition has been demonstrated in [6] for the solution of fluid flow problems.

4.3. Condition number estimates. Depending on the type of solution method applied to (10) after Lagrangian augmentation, some or all of the spectral condition numbers of $\widetilde{\boldsymbol{A}}_{\gamma\boldsymbol{W}}$, $\boldsymbol{A}_{\gamma\boldsymbol{W}}$, and $\boldsymbol{S}_{\gamma\boldsymbol{W}}$ are of interest. General condition number bounds

for Lagrangian augmentation can be found in [13, 10], but in our case the analysis simplifies because $\boldsymbol{A}_{\gamma\boldsymbol{W}}$ and $\boldsymbol{S}_{\gamma\boldsymbol{W}}$ can be made positive and negative definite, respectively, by choosing γ large enough.

First, we will derive a bound on $\kappa_2(\widetilde{\boldsymbol{A}}_{\gamma\boldsymbol{W}})$ which is quadratic in γ. Similar bounds can be found in [13, p. 2079] and [10, p. 5]. For the proof of the following theorem note that for $\widetilde{\boldsymbol{N}}_{\gamma\boldsymbol{W}}$ from (11) we have

$$\|\widetilde{\boldsymbol{N}}_{\gamma\boldsymbol{W}}\|_2 \le 1 + \gamma\|\boldsymbol{B}\boldsymbol{W}\|_2. \tag{22}$$

THEOREM 4. *Assume that $\boldsymbol{A}_{\gamma_0\boldsymbol{W}}$ is positive definite for some $\gamma_0 \ge 0$. Then $\boldsymbol{A}_{\gamma\boldsymbol{W}}$ is positive definite for all $\gamma \ge \gamma_0$, and it holds that*

$$\kappa_2(\widetilde{\boldsymbol{A}}_{\gamma\boldsymbol{W}}) \le (1 + (\gamma - \gamma_0)\|\boldsymbol{B}\boldsymbol{W}\|_2)^2\, \kappa_2(\widetilde{\boldsymbol{A}}_{\gamma_0\boldsymbol{W}}). \tag{23}$$

Proof. Based on (22) and using $\widetilde{\boldsymbol{N}}^{-1}_{(\gamma-\gamma_0)\boldsymbol{W}} = \widetilde{\boldsymbol{N}}_{(\gamma_0-\gamma)\boldsymbol{W}}$ from (11), we have

$$\begin{aligned}
\widetilde{\boldsymbol{A}}_{\gamma\boldsymbol{W}} = \widetilde{\boldsymbol{N}}_{(\gamma-\gamma_0)\boldsymbol{W}}\widetilde{\boldsymbol{A}}_{\gamma_0\boldsymbol{W}} \quad &\Rightarrow \quad \|\widetilde{\boldsymbol{A}}_{\gamma\boldsymbol{W}}\|_2 \le (1 + (\gamma - \gamma_0)\|\boldsymbol{B}\boldsymbol{W}\|_2)\|\widetilde{\boldsymbol{A}}_{\gamma_0\boldsymbol{W}}\|_2,\\
\widetilde{\boldsymbol{A}}^{-1}_{\gamma\boldsymbol{W}} = \widetilde{\boldsymbol{A}}^{-1}_{\gamma_0\boldsymbol{W}}\widetilde{\boldsymbol{N}}_{(\gamma_0-\gamma)\boldsymbol{W}} \quad &\Rightarrow \quad \|\widetilde{\boldsymbol{A}}^{-1}_{\gamma\boldsymbol{W}}\|_2 \le (1 + (\gamma - \gamma_0)\|\boldsymbol{B}\boldsymbol{W}\|_2)\|\widetilde{\boldsymbol{A}}^{-1}_{\gamma_0\boldsymbol{W}}\|_2.
\end{aligned}$$

Now (23) follows from $\kappa_2(\widetilde{\boldsymbol{A}}_{\gamma\boldsymbol{W}}) = \|\widetilde{\boldsymbol{A}}_{\gamma\boldsymbol{W}}\|_2\|\widetilde{\boldsymbol{A}}^{-1}_{\gamma\boldsymbol{W}}\|_2$ ∎

For $\kappa_2(\boldsymbol{A}_{\gamma\boldsymbol{W}})$ and $\kappa_2(\boldsymbol{S}_{\gamma\boldsymbol{W}})$ we will make use of the following lemma.

LEMMA 5. *Assume that $\boldsymbol{A} \in \mathbb{R}^{N\times N}$ is positive definite and $\boldsymbol{M} \in \mathbb{R}^{N\times N}$ is positive semidefinite. Then for $\mu \ge 0$ it holds that*

$$\kappa_2(\boldsymbol{A} + \mu\boldsymbol{M}) \le \kappa_2(\boldsymbol{A}) + \mu\|\boldsymbol{M}\|_2\|\boldsymbol{A}^{-1}\|_2. \tag{24}$$

Proof. Since $\boldsymbol{A}$ and $\boldsymbol{M}$ are symmetric matrices, we have

$$\begin{aligned}
\lambda_{\max}(\boldsymbol{A} + \mu\boldsymbol{M}) &\le \lambda_{\max}(\boldsymbol{A}) + \mu\lambda_{\max}(\boldsymbol{M}),\\
\lambda_{\min}(\boldsymbol{A} + \mu\boldsymbol{M}) &\ge \lambda_{\min}(\boldsymbol{A}) + \mu\lambda_{\min}(\boldsymbol{M}) \ge \lambda_{\min}(\boldsymbol{A}).
\end{aligned}$$

The result follows from

$$\kappa_2(\boldsymbol{A} + \mu\boldsymbol{M}) = \frac{\lambda_{\max}(\boldsymbol{A} + \mu\boldsymbol{M})}{\lambda_{\min}(\boldsymbol{A} + \mu\boldsymbol{M})} \le \frac{\lambda_{\max}(\boldsymbol{A}) + \mu\lambda_{\max}(\boldsymbol{M})}{\lambda_{\min}(\boldsymbol{A})} \le \kappa_2(\boldsymbol{A}) + \mu\frac{\lambda_{\max}(\boldsymbol{M})}{\lambda_{\min}(\boldsymbol{A})}$$

since $\lambda_{\max}(\boldsymbol{M}) = \|\boldsymbol{M}\|_2$ and $\lambda_{\min}(\boldsymbol{A}) = 1/\|\boldsymbol{A}^{-1}\|_2$. ∎

We can use Lemma 5 to show that $\kappa_2(\boldsymbol{A}_{\gamma\boldsymbol{W}})$ scales only linearly with respect to γ.

THEOREM 6. *Assume that $\boldsymbol{A}_{\gamma_0\boldsymbol{W}}$ is positive definite for some $\gamma_0 \ge 0$. Then, for all $\gamma \ge \gamma_0$, it holds that*

$$\kappa_2(\boldsymbol{A}_{\gamma\boldsymbol{W}}) \le \kappa_2(\boldsymbol{A}_{\gamma_0\boldsymbol{W}}) + (\gamma - \gamma_0)\frac{\lambda_{\max}(\boldsymbol{B}\boldsymbol{W}\boldsymbol{B}^{\mathsf{T}})}{\lambda_{\min}(\boldsymbol{A}_{\gamma_0\boldsymbol{W}})}. \tag{25}$$

Proof. The proposition follows using Lemma 5 with $\boldsymbol{A} := \boldsymbol{A}_{\gamma_0\boldsymbol{W}}$ and $\boldsymbol{M} := (\gamma - \gamma_0)\boldsymbol{B}\boldsymbol{W}\boldsymbol{B}^{\mathsf{T}}$. ∎

Remark 7. For $\boldsymbol{B} = \boldsymbol{Q}\boldsymbol{R}$ and $\boldsymbol{W} = \boldsymbol{R}^{-1}\boldsymbol{R}^{-\mathsf{T}}$, the bound (25) simplifies to

$$\kappa_2(\boldsymbol{A}_{\gamma\boldsymbol{W}}) \le \kappa_2(\boldsymbol{A}_{\gamma_0\boldsymbol{W}}) + (\gamma - \gamma_0)\|\boldsymbol{A}^{-1}_{\gamma_0\boldsymbol{W}}\|_2.$$

In order to bound $\kappa_2(\boldsymbol{S}_{\gamma\boldsymbol{W}})$ we use the following representation of $\boldsymbol{S}_{\gamma\boldsymbol{W}}^{-1}$.

LEMMA 8. *Assume that $\boldsymbol{A}_{\gamma_0\boldsymbol{W}}$ is positive definite for some $\gamma_0 \geq 0$. Then for $\gamma \geq \gamma_0$, the inverse of the negative definite $\boldsymbol{S}_{\gamma\boldsymbol{W}}$ is*

$$\boldsymbol{S}_{\gamma\boldsymbol{W}}^{-1} = \boldsymbol{S}_{\gamma_0\boldsymbol{W}}^{-1} - (\gamma - \gamma_0)\boldsymbol{W}. \tag{26}$$

Proof. This relation between $\boldsymbol{S}_{\gamma\boldsymbol{W}}^{-1}$ and $\boldsymbol{S}_{\gamma_0\boldsymbol{W}}^{-1}$ in (26) can be found in [13, Proposition 2.1] or [4, Lemma 4.1]. ∎

THEOREM 9. *Assume that $\boldsymbol{A}_{\gamma_0\boldsymbol{W}}$ is positive definite for some $\gamma_0 \geq 0$. Then for $\gamma \geq \gamma_0$, it holds that*

$$\kappa_2(\boldsymbol{S}_{\gamma\boldsymbol{W}}) \leq \kappa_2(\boldsymbol{S}_{\gamma_0\boldsymbol{W}}) + (\gamma - \gamma_0)\|\boldsymbol{W}\|_2\|\boldsymbol{S}_{\gamma_0\boldsymbol{W}}\|_2, \tag{27}$$

$$\kappa_2(\boldsymbol{S}_{\gamma\boldsymbol{W}}) \leq \kappa_2(\boldsymbol{W}) + \frac{1}{\gamma - \gamma_0}\|\boldsymbol{W}^{-1}\|_2\|\boldsymbol{S}_{\gamma_0\boldsymbol{W}}^{-1}\|_2 \tag{28}$$

and $\kappa_2(\boldsymbol{S}_{\gamma\boldsymbol{W}}) \to \kappa_2(\boldsymbol{W})$ as $\gamma \to \infty$.

Proof. The proof follows from Lemmas 8 and 5 using $\kappa_2(\boldsymbol{S}_{\gamma\boldsymbol{W}}^{-1}) = \kappa_2(\boldsymbol{S}_{\gamma\boldsymbol{W}})$. ∎

5. Nullspace method. Using a matrix $\boldsymbol{C} \in \mathbb{R}^{N\times(N-M)}$ with columns spanning the nullspace of $\boldsymbol{B}^\mathsf{T}$, every $\boldsymbol{\alpha} \in \ker(\boldsymbol{B}^\mathsf{T})$ can be written as $\boldsymbol{\alpha} = \boldsymbol{C}\boldsymbol{\alpha}'$ for some $\boldsymbol{\alpha}' \in \mathbb{R}^{N-M}$. The representation of $\boldsymbol{\alpha}$ in terms of the nullspace basis $\boldsymbol{C}$ can be used to make the constraint $\boldsymbol{B}^\mathsf{T}\boldsymbol{\alpha} = \boldsymbol{0}$ in (1) implicit. Substituting $\boldsymbol{\alpha} = \boldsymbol{C}\boldsymbol{\alpha}'$ into the first block row of (1) leads to

$$\boldsymbol{A}\boldsymbol{C}\boldsymbol{\alpha}' + \boldsymbol{B}\boldsymbol{\beta} = \boldsymbol{f}. \tag{29}$$

Multiplication of (29) by $\boldsymbol{C}^\mathsf{T}$ eliminates the polynomial coefficients and yields

$$\boldsymbol{C}^\mathsf{T}\boldsymbol{A}\boldsymbol{C}\boldsymbol{\alpha}' = \boldsymbol{C}^\mathsf{T}\boldsymbol{f} \quad \Leftrightarrow: \quad \boldsymbol{A}'\boldsymbol{\alpha}' = \boldsymbol{f}'. \tag{30}$$

The projected main block $\boldsymbol{A}' = \boldsymbol{C}^\mathsf{T}\boldsymbol{A}\boldsymbol{C} \in \mathbb{R}^{(N-M)\times(N-M)}$ is positive definite because $\boldsymbol{A}$ is positive definite on $\ker(\boldsymbol{B}^\mathsf{T})$. The RBF coefficients $\boldsymbol{\alpha}$ can be found by solving (30) for $\boldsymbol{\alpha}'$, e.g., using the CG algorithm with $\mathcal{H}$-Cholesky preconditioning. After recovering $\boldsymbol{\alpha} = \boldsymbol{C}\boldsymbol{\alpha}'$, the polynomial coefficients $\boldsymbol{\beta}$ can be computed from $\boldsymbol{B}\boldsymbol{\beta} = \boldsymbol{f} - \boldsymbol{A}\boldsymbol{\alpha}$, an overdetermined system which is consistent by construction.

5.1. Preconditioning interpretation. The nullspace method can be interpreted as a block preconditioner for (1), leading to a blockwise antitriangular factorization of $\widetilde{\boldsymbol{A}}$ as described in [21, 22]. Recently, variants of this factorization have been compared in [24] for the case of sparse matrices $\boldsymbol{A}$, $\boldsymbol{B}$.

Since $\boldsymbol{C} \in \mathbb{R}^{N\times(N-M)}$ is assumed to have full rank, there exists an $\boldsymbol{E} \in \mathbb{R}^{N\times M}$ such that $\boldsymbol{D} = (\boldsymbol{E}, \boldsymbol{C}) \in \mathbb{R}^{N\times N}$ is invertible and $\mathrm{im}(\boldsymbol{E}) = \mathrm{im}(\boldsymbol{B})$. We then have

$$\boldsymbol{D}^\mathsf{T}\boldsymbol{B} = (\boldsymbol{E}, \boldsymbol{C})^\mathsf{T}\boldsymbol{B} = \begin{pmatrix} \boldsymbol{E}^\mathsf{T}\boldsymbol{B} \\ \boldsymbol{C}^\mathsf{T}\boldsymbol{B} \end{pmatrix} =: \begin{pmatrix} \boldsymbol{R}_1 \\ \boldsymbol{O} \end{pmatrix} =: \boldsymbol{R}, \tag{31}$$

where $\boldsymbol{R}_1 \in \mathbb{R}^{M\times M}$ is invertible since $\boldsymbol{D}$ and $\boldsymbol{B}$ have full rank. The invertibility of $\boldsymbol{D}$ allows for a two-sided preconditioning of $\widetilde{\boldsymbol{A}}$ to obtain the antitriangular matrix

$$\widetilde{\boldsymbol{D}}^\mathsf{T}\,\widetilde{\boldsymbol{A}}\,\widetilde{\boldsymbol{D}} = \begin{pmatrix} * & * & \boldsymbol{R}_1 \\ * & \boldsymbol{C}^\mathsf{T}\boldsymbol{A}\boldsymbol{C} & \boldsymbol{O} \\ \boldsymbol{R}_1^\mathsf{T} & \boldsymbol{O} & \boldsymbol{O} \end{pmatrix} \quad \text{with} \quad \widetilde{\boldsymbol{D}} := \begin{pmatrix} \boldsymbol{D} & \boldsymbol{O} \\ \boldsymbol{O} & \boldsymbol{I}_M \end{pmatrix}. \tag{32}$$

Based on (32), the linear system (1) can be solved by back-substitution which amounts to the same computational steps as in the "traditional" formulation of the nullspace method.

5.2. Condition number bounds. Since $\boldsymbol{A}' = \boldsymbol{C}^\mathsf{T}\boldsymbol{A}\boldsymbol{C}$ constitutes the largest block in (32), its condition number is of special importance and depends on the condition number $\kappa_2(\boldsymbol{C}) = \frac{\sigma_{\max}(\boldsymbol{C})}{\sigma_{\min}(\boldsymbol{C})}$ of the rectangular matrix $\boldsymbol{C} \in \mathbb{R}^{N\times(N-M)}$. The extremal singular values of $\boldsymbol{C}$ satisfy

$$\sigma_{\max}(\boldsymbol{C}) = \max_{\|\boldsymbol{y}\|_2=1} \|\boldsymbol{C}\boldsymbol{y}\|_2, \quad \sigma_{\min}(\boldsymbol{C}) = \min_{\|\boldsymbol{y}\|_2=1} \|\boldsymbol{C}\boldsymbol{y}\|_2.$$

Note that the characterization of the largest singular value holds for matrices of any shape while the characterization of the smallest singular value relies on the fact that the number of columns of $\boldsymbol{C}$ is less than or equal to the number of rows.

THEOREM 10. *The condition number of $\boldsymbol{A}' = \boldsymbol{C}^\mathsf{T}\boldsymbol{A}\boldsymbol{C}$ is bounded by*

$$\kappa_2(\boldsymbol{A}') \le \kappa_2(\widetilde{\boldsymbol{A}})\, \kappa_2(\boldsymbol{C})^2. \tag{33}$$

Proof. In order to derive a lower bound for $\sigma_{\min}(\boldsymbol{C}^\mathsf{T}\boldsymbol{A}\boldsymbol{C})$, we begin with

$$\begin{aligned}
\sigma_{\min}(\boldsymbol{C}^\mathsf{T}\boldsymbol{A}\boldsymbol{C}) &= \lambda_{\min}(\boldsymbol{C}^\mathsf{T}\boldsymbol{A}\boldsymbol{C}) \\
&= \min\left\{\boldsymbol{\alpha}'^\mathsf{T}(\boldsymbol{C}^\mathsf{T}\boldsymbol{A}\boldsymbol{C})\boldsymbol{\alpha}' \mid \|\boldsymbol{\alpha}'\|_2 = 1\right\} \\
&= \min\left\{(\boldsymbol{C}\boldsymbol{\alpha}')^\mathsf{T}\boldsymbol{A}(\boldsymbol{C}\boldsymbol{\alpha}') \mid \|\boldsymbol{\alpha}'\|_2 \ge 1\right\} \\
&\ge \min\left\{\boldsymbol{\alpha}^\mathsf{T}\boldsymbol{A}\boldsymbol{\alpha} \mid \|\boldsymbol{\alpha}\|_2 \ge \sigma_{\min}(\boldsymbol{C}),\ \boldsymbol{\alpha} \in \ker(\boldsymbol{B}^\mathsf{T})\right\},
\end{aligned} \tag{34}$$

where we have replaced $\boldsymbol{C}\boldsymbol{\alpha}'$ with $\boldsymbol{\alpha}$ in the last step. From $\|\boldsymbol{\alpha}'\|_2 \ge 1$, it follows that $\|\boldsymbol{C}\boldsymbol{\alpha}'\|_2 \ge \sigma_{\min}(\boldsymbol{C})$, and since $\boldsymbol{C}$ is a basis for $\ker(\boldsymbol{B}^\mathsf{T})$ it holds that $\boldsymbol{C}\boldsymbol{\alpha}' \in \ker(\boldsymbol{B}^\mathsf{T})$. Therefore, the inequality in the last line of (34) follows from the set inclusion

$$\{\boldsymbol{C}\boldsymbol{\alpha}' \mid \|\boldsymbol{\alpha}'\|_2 \ge 1,\ \boldsymbol{\alpha}' \in \mathbb{R}^{N-M}\} \subseteq \{\boldsymbol{\alpha} \mid \|\boldsymbol{\alpha}\|_2 \ge \sigma_{\min}(\boldsymbol{C}),\ \boldsymbol{\alpha} \in \ker(\boldsymbol{B}^\mathsf{T})\}.$$

Continuing from (34), we get

$$\sigma_{\min}(\boldsymbol{C}^\mathsf{T}\boldsymbol{A}\boldsymbol{C}) \ge \lambda^+_{\min}(\boldsymbol{A})\, \sigma_{\min}(\boldsymbol{C})^2 \ge \sigma_{\min}(\widetilde{\boldsymbol{A}})\, \sigma_{\min}(\boldsymbol{C})^2, \tag{35}$$

where $\lambda^+_{\min}(\boldsymbol{A})$ denotes the smallest *positive* eigenvalue of $\boldsymbol{A}$. The first inequality in (35) follows from (34) because $\boldsymbol{A}$ is positive definite on $\ker(\boldsymbol{B}^\mathsf{T})$. For the last inequality in (35), we make use of $\lambda^+_{\min}(\boldsymbol{A}) \ge \sigma_{\min}(\widetilde{\boldsymbol{A}})$ because $\boldsymbol{A}$ is a diagonal block of $\widetilde{\boldsymbol{A}}$. Similarly, as an upper bound for $\sigma_{\max}(\boldsymbol{C}^\mathsf{T}\boldsymbol{A}\boldsymbol{C})$) we have

$$\begin{aligned}
\sigma_{\max}(\boldsymbol{C}^\mathsf{T}\boldsymbol{A}\boldsymbol{C}) &= \lambda_{\max}(\boldsymbol{C}^\mathsf{T}\boldsymbol{A}\boldsymbol{C}) \\
&= \max\left\{\boldsymbol{\alpha}'^\mathsf{T}(\boldsymbol{C}^\mathsf{T}\boldsymbol{A}\boldsymbol{C})\boldsymbol{\alpha}' \mid \|\boldsymbol{\alpha}'\|_2 = 1\right\} \\
&= \max\left\{(\boldsymbol{C}\boldsymbol{\alpha}')^\mathsf{T}\boldsymbol{A}(\boldsymbol{C}\boldsymbol{\alpha}') \mid \|\boldsymbol{\alpha}'\|_2 \le 1\right\} \\
&\le \max\left\{\boldsymbol{\alpha}^\mathsf{T}\boldsymbol{A}\boldsymbol{\alpha} \mid \|\boldsymbol{\alpha}\|_2 \le \sigma_{\max}(\boldsymbol{C}),\ \boldsymbol{\alpha} \in \ker(\boldsymbol{B}^\mathsf{T})\right\} \\
&\le \lambda_{\max}(\boldsymbol{A})\, \sigma_{\max}(\boldsymbol{C})^2 \\
&\le \sigma_{\max}(\widetilde{\boldsymbol{A}})\, \sigma_{\max}(\boldsymbol{C})^2
\end{aligned} \tag{36}$$

such that (33) follows from

$$\kappa_2(\boldsymbol{C}^\mathsf{T}\boldsymbol{A}\boldsymbol{C}) = \frac{\sigma_{\max}(\boldsymbol{C}^\mathsf{T}\boldsymbol{A}\boldsymbol{C})}{\sigma_{\min}(\boldsymbol{C}^\mathsf{T}\boldsymbol{A}\boldsymbol{C})} \le \frac{\sigma_{\max}(\widetilde{\boldsymbol{A}})\, \sigma_{\max}(\boldsymbol{C})^2}{\sigma_{\min}(\widetilde{\boldsymbol{A}})\, \sigma_{\min}(\boldsymbol{C})^2} = \kappa_2(\widetilde{\boldsymbol{A}})\, \kappa_2(\boldsymbol{C})^2$$

by combining (35) and (36). ∎

5.3. Nullspace construction. All that is needed in the transformation of $\widetilde{\boldsymbol{A}}$ to antitriangular form (32) is to find an invertible matrix $\boldsymbol{D}$ such that $\boldsymbol{D}^{\mathsf{T}}\boldsymbol{B} = \boldsymbol{R}$ is zero in its last $(N-M)$ rows. Suitable $\boldsymbol{D}$ and $\boldsymbol{R}$ can be obtained from any decomposition $\boldsymbol{B} = \boldsymbol{D}^{-\mathsf{T}}\boldsymbol{R}$, where $\boldsymbol{R}$ is upper triangular. We will consider an LU factorization $\boldsymbol{B} = \boldsymbol{L}\boldsymbol{R}$ giving $\boldsymbol{D} = \boldsymbol{L}^{-\mathsf{T}}$ in section 5.4 and a QR factorization $\boldsymbol{B} = \boldsymbol{Q}\boldsymbol{R}$, where $\boldsymbol{D} = \boldsymbol{Q}^{-\mathsf{T}} = \boldsymbol{Q}$, in section 5.6.

5.4. Nullspace construction via LU decomposition. In this section, we investigate the construction of the nullspace basis $\boldsymbol{C}$ using an LU decomposition $\boldsymbol{B} = \boldsymbol{L}\boldsymbol{R}$, where $\boldsymbol{L}$ is unit lower triangular. To assure that the factorization $\boldsymbol{B} = \boldsymbol{L}\boldsymbol{R}$ is stable, we assume that the rows of $\boldsymbol{B}$ have been ordered appropriately before the factorization is performed. This is achieved by performing a pivoted LU factorization $\boldsymbol{P}\boldsymbol{B} = \boldsymbol{L}\boldsymbol{R}$, where $\boldsymbol{P}$ describes the permutation of rows resulting from pivoting. Then the original $\boldsymbol{B}$ is replaced by $\boldsymbol{P}\boldsymbol{B}$ and the pivoted LU decomposition is written as $\boldsymbol{B} = \boldsymbol{L}\boldsymbol{R}$ as in the nonpivoted case. This allows us to describe the construction of $\boldsymbol{C}$ in terms of the blocks of $\boldsymbol{L}$ without further reference to the permutation matrix $\boldsymbol{P}$. Since the permutation $\boldsymbol{P}$ corresponds to a reordering of the scattered centers $\boldsymbol{x}_1, \ldots, \boldsymbol{x}_N$, the main block $\boldsymbol{A}$ within the saddle-point matrix $\widetilde{\boldsymbol{A}}$ is also replaced by $\boldsymbol{P}\boldsymbol{A}\boldsymbol{P}^{\mathsf{T}}$. Finally, the right-hand side $\boldsymbol{f}$ is replaced by $\boldsymbol{P}\boldsymbol{f}$ as well; i.e., the pivoting process amounts to a two-sided preconditioning of the original linear system (1).

We will discuss partial pivoting and its effect on the condition number of $\boldsymbol{C}$ in section 5.5.

In order to obtain $\boldsymbol{C}$ from $\boldsymbol{D} = \boldsymbol{L}^{-\mathsf{T}} = (\boldsymbol{E}, \boldsymbol{C})$, we partition $\boldsymbol{B} = \boldsymbol{L}\boldsymbol{R}$ into

$$\begin{pmatrix} \boldsymbol{B}_1 \\ \boldsymbol{B}_2 \end{pmatrix} = \begin{pmatrix} \boldsymbol{L}_{1,1} & \boldsymbol{O} \\ \boldsymbol{L}_{2,1} & \boldsymbol{I}_{N-M} \end{pmatrix} \begin{pmatrix} \boldsymbol{R}_1 \\ \boldsymbol{O} \end{pmatrix}, \tag{37}$$

where $\boldsymbol{B}_1, \boldsymbol{L}_{1,1}, \boldsymbol{R}_1 \in \mathbb{R}^{M \times M}$ are small square matrices and $\boldsymbol{L}_{2,2} = \boldsymbol{I}_{N-M}$ is an identity matrix of order $N - M$. Since (37) is equivalent to

$$\boldsymbol{B}_1 = \boldsymbol{L}_{1,1}\boldsymbol{R}_1, \qquad \boldsymbol{B}_2 = \boldsymbol{L}_{2,1}\boldsymbol{R}_1,$$

the blocks from (37) are defined in terms of an LU factorization of $\boldsymbol{B}_1$ and an upper triangular solve giving $\boldsymbol{L}_{2,1} = \boldsymbol{B}_2\boldsymbol{R}_1^{-1}$.

For the inverse of $\boldsymbol{L}$, we write $\widetilde{\boldsymbol{L}} = \boldsymbol{L}^{-1}$ with blocks

$$\widetilde{\boldsymbol{L}} = \begin{pmatrix} \boldsymbol{L}_{1,1}^{-1} & \boldsymbol{O} \\ \widetilde{\boldsymbol{L}}_{2,1} & \boldsymbol{I}_{N-M} \end{pmatrix}, \quad \widetilde{\boldsymbol{L}}_{2,1} = -\boldsymbol{L}_{2,1}\boldsymbol{L}_{1,1}^{-1} \in \mathbb{R}^{(N-M)\times M}. \tag{38}$$

From (38), together with $\widetilde{\boldsymbol{L}}^{\mathsf{T}} = (\boldsymbol{E}, \boldsymbol{C})$, we get the sparse nullspace basis $\boldsymbol{C}$, often referred to as the fundamental basis [24, eq. (6)], as

$$\boldsymbol{C} = \begin{pmatrix} \widetilde{\boldsymbol{L}}_{2,1}^{\mathsf{T}} \\ \boldsymbol{I}_{N-M} \end{pmatrix} \in \mathbb{R}^{N \times (N-M)}. \tag{39}$$

Based on the blocks of $\widetilde{\boldsymbol{L}}$, the computation of $\boldsymbol{A}^{\mathrm{LU}} := \boldsymbol{D}^{\mathsf{T}}\boldsymbol{A}\boldsymbol{D}$ in (32) is carried out as

$$\boldsymbol{A}^{\mathrm{LU}} = \widetilde{\boldsymbol{L}}\boldsymbol{A}\widetilde{\boldsymbol{L}}^{\mathsf{T}} = \begin{pmatrix} \boldsymbol{L}_{1,1}^{-1} & \boldsymbol{O} \\ \widetilde{\boldsymbol{L}}_{2,1} & \boldsymbol{I}_{N-M} \end{pmatrix} \begin{pmatrix} \boldsymbol{A}_{1,1} & \boldsymbol{A}_{1,2} \\ \boldsymbol{A}_{2,1} & \boldsymbol{A}_{2,2} \end{pmatrix} \begin{pmatrix} \boldsymbol{L}_{1,1}^{-\mathsf{T}} & \widetilde{\boldsymbol{L}}_{2,1}^{\mathsf{T}} \\ \boldsymbol{O} & \boldsymbol{I}_{N-M} \end{pmatrix}. \tag{40}$$

Here, the individual blocks of $\boldsymbol{A}^{\mathrm{LU}}$ are

$$
\begin{aligned}
\boldsymbol{A}_{1,1}^{\mathrm{LU}} &= \boldsymbol{L}_{1,1}^{-1}\boldsymbol{A}_{1,1}\boldsymbol{L}_{1,1}^{-\mathsf{T}} \in \mathbb{R}^{M\times M},\\
\boldsymbol{A}_{1,2}^{\mathrm{LU}} &= (\boldsymbol{A}_{2,1}^{\mathrm{LU}})^{\mathsf{T}} = \boldsymbol{L}_{1,1}^{-1}(\boldsymbol{A}_{1,1}\widetilde{\boldsymbol{L}}_{2,1}^{\mathsf{T}} + \boldsymbol{A}_{1,2}) \in \mathbb{R}^{(N-M)\times M},\\
\boldsymbol{A}_{2,2}^{\mathrm{LU}} &= \boldsymbol{A}_{2,2} + \widetilde{\boldsymbol{L}}_{2,1}\boldsymbol{A}_{1,1}\widetilde{\boldsymbol{L}}_{2,1}^{\mathsf{T}} + \widetilde{\boldsymbol{L}}_{2,1}\boldsymbol{A}_{1,2} + \boldsymbol{A}_{2,1}\widetilde{\boldsymbol{L}}_{2,1}^{\mathsf{T}}\\
&= \boldsymbol{A}_{2,2} + \begin{pmatrix}\widetilde{\boldsymbol{L}}_{2,1} & \boldsymbol{A}_{2,1}\end{pmatrix}\begin{pmatrix}\boldsymbol{A}_{1,1} & \boldsymbol{I}_M\\ \boldsymbol{I}_M & \boldsymbol{O}\end{pmatrix}\begin{pmatrix}\widetilde{\boldsymbol{L}}_{2,1} & \boldsymbol{A}_{2,1}\end{pmatrix}^{\mathsf{T}}\\
&= \boldsymbol{A}_{2,2} + \begin{pmatrix}\widetilde{\boldsymbol{L}}_{2,1}\boldsymbol{A}_{1,1} + \boldsymbol{A}_{2,1} & \widetilde{\boldsymbol{L}}_{2,1}\end{pmatrix}\begin{pmatrix}\widetilde{\boldsymbol{L}}_{2,1} & \boldsymbol{A}_{2,1}\end{pmatrix}^{\mathsf{T}} \in \mathbb{R}^{(N-M)\times(N-M)};
\end{aligned}
\tag{41}
$$

i.e., $\boldsymbol{A}_{2,2}^{\mathrm{LU}}$ is a rank-$2M$ update of $\boldsymbol{A}_{2,2}$ within the arithmetics of $\mathcal{H}$-matrices. The small $\boldsymbol{A}_{1,1}^{\mathrm{LU}}$ (if needed) and $\boldsymbol{A}_{1,2}^{\mathrm{LU}}$ can be set up in full.

5.5. Pivoting strategy. We use partial pivoting [17, section 9] to assure that in $\boldsymbol{B} = \boldsymbol{L}\boldsymbol{R}$, each entry $L_{i,j}$ of $\boldsymbol{L}$ is bounded by one in magnitude,

$$
|L_{i,j}| \le 1, \quad i,j = 1,\dots,N. \tag{42}
$$

The action of the permutation matrix $\boldsymbol{P}$ on the rows of $\boldsymbol{B}$ as described in section 5.4 can be thought of as selecting a special subset of M centers from $X = \{\boldsymbol{x}_1,\dots,\boldsymbol{x}_N\}$. After the permutation has been applied, these pivot centers are the first M centers $\boldsymbol{x}_1,\dots,\boldsymbol{x}_M$ of X and correspond to the first M rows of $\boldsymbol{B}_1$. As far as the pivoting process is concerned, the remaining $N-M$ centers of X can be assigned to the rows of $\boldsymbol{B}_2$ in abitrary order to ensure that the entries of $\boldsymbol{L}$ are bounded as in (42).

An illustration of these pivot centers $\boldsymbol{x}_1,\dots,\boldsymbol{x}_M$ obtained from partial pivoting using polynomial degrees $m = 3,4,5,6$ is given in Figure 2. Visually, the pivoting process resembles the selection of M coarse grid centers which are distributed throughout the domain which in this example is a unit disc in $\mathbb{R}^2$.

We conclude the discussion of the nullspace construction via LU decomposition by deriving bounds on the spectral condition numbers of the nullspace basis $\boldsymbol{C}$ and the projected main block $\boldsymbol{A}' = \boldsymbol{C}^{\mathsf{T}}\boldsymbol{A}\boldsymbol{C}$.

THEOREM 11. *The construction of the nullspace basis $\boldsymbol{C}$ via LU factorization with partial pivoting results in*

$$
\kappa_2(\boldsymbol{C}) \le \sqrt{1+2^{2M}M^2N} \le 1+M2^M\sqrt{N}, \qquad \kappa_2(\boldsymbol{A}') \le (1+M^2 2^{2M}N)\cdot\kappa_2(\widetilde{\boldsymbol{A}}), \tag{43}
$$

with $\boldsymbol{A}'$ and $\widetilde{\boldsymbol{A}}$ defined in (30), (1), *respectively.*

Proof. We start with $\kappa_2(\boldsymbol{C})$ after which we can use Theorem 10 for $\kappa_2(\boldsymbol{A}')$. For the smallest singular value of $\boldsymbol{C}$, the blockwise representation from (39) leads to

$$
\|\boldsymbol{C}\boldsymbol{\alpha}'\|_2 = \left\|\begin{pmatrix}-\boldsymbol{L}_{1,1}^{-\mathsf{T}}\boldsymbol{L}_{2,1}^{\mathsf{T}}\boldsymbol{\alpha}'\\ \boldsymbol{\alpha}'\end{pmatrix}\right\|_2 \ge \|\boldsymbol{\alpha}'\|_2 \quad\Rightarrow\quad \sigma_{\min}(\boldsymbol{C}) \ge 1. \tag{44}
$$

In order to bound the largest singular value of $\boldsymbol{C}$, we start with

$$
\|\boldsymbol{C}\boldsymbol{\alpha}'\|_2 = \sqrt{\|\boldsymbol{\alpha}'\|_2^2 + \|\boldsymbol{L}_{1,1}^{-\mathsf{T}}\boldsymbol{L}_{2,1}^{\mathsf{T}}\boldsymbol{\alpha}'\|_2^2} \le \sqrt{1+\|\boldsymbol{L}_{1,1}^{-\mathsf{T}}\|_2^2\,\|\boldsymbol{L}_{2,1}^{\mathsf{T}}\|_2^2}\cdot\|\boldsymbol{\alpha}'\|_2. \tag{45}
$$

Based on the discussion of partial pivoting in [17, Chapter 9.4] and [18, eq. (2.6)] or a simple inductive proof, we know that

$$
\|\boldsymbol{L}_{1,1}^{-\mathsf{T}}\|_\infty \le 2^M, \tag{46}
$$

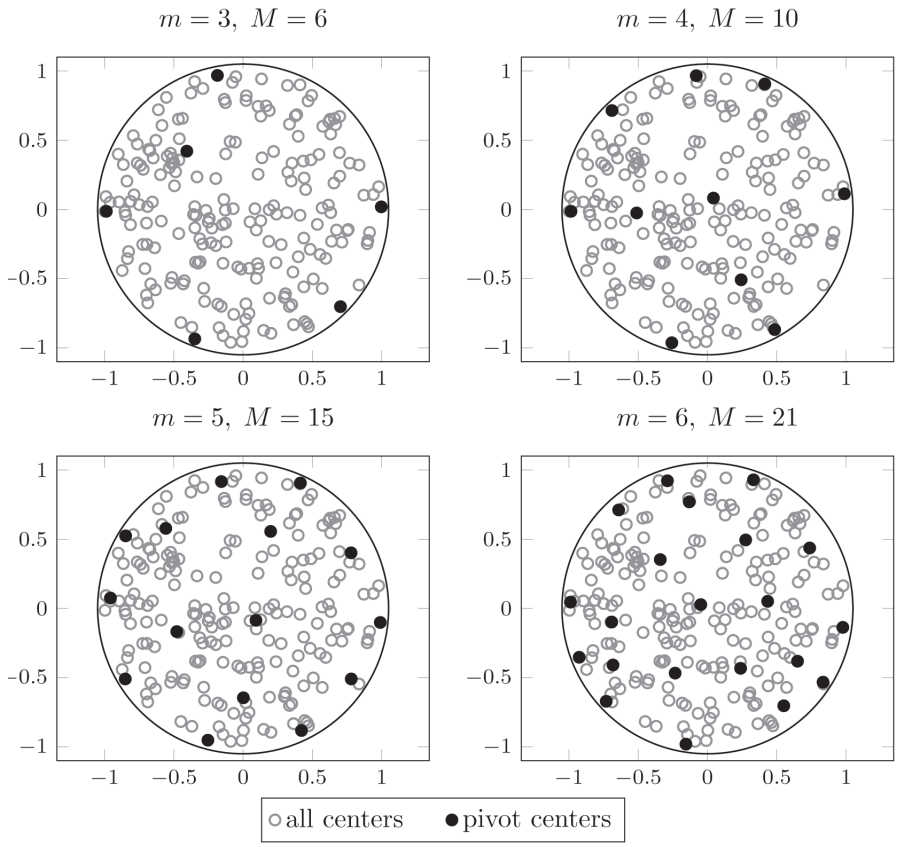

FIG. 2. *Selection of pivot centers out of a set of $N = 200$ random centers from a uniform distribution in a (two-dimensional) disc. The polynomial degree was chosen as $m = 3, 4, 5, 6$ corresponding to $M = 6, 10, 15, 21$ pivot centers.*

and hence the Euclidean norm of $\boldsymbol{L}_{1,1}^{-\mathsf{T}}$ is bounded by

$$\|\boldsymbol{L}_{1,1}^{-\mathsf{T}}\|_2 \leq \sqrt{M}\ \|\boldsymbol{L}_{1,1}^{-\mathsf{T}}\|_\infty \leq 2^M\ \sqrt{M}. \tag{47}$$

Since $\boldsymbol{L}_{2,1} \in \mathbb{R}^{(N-M)\times M}$ has $(N-M)M$ entries which satisfy $|L_{i,j}| \leq 1$ (42), its Frobenius norm is bounded by $\|\boldsymbol{L}_{2,1}\|_{\mathrm{F}} \leq \sqrt{M(N-M)}$ and hence its Euclidean norm is bounded by

$$\|\boldsymbol{L}_{2,1}\|_2 \leq \|\boldsymbol{L}_{2,1}\|_{\mathrm{F}} \leq \sqrt{MN}. \tag{48}$$

Starting from (45), the application of the bounds (47) and (48) results in

$$\|\boldsymbol{C}\boldsymbol{\alpha}'\|_2 \leq \sqrt{1 + 2^{2M} M^2 N} \cdot \|\boldsymbol{\alpha}'\|_2$$

such that the largest singular value of $\boldsymbol{C}$ is bounded by

$$\sigma_{\max}(\boldsymbol{C}) \leq \sqrt{1 + 2^{2M} M^2 N} \leq 1 + M 2^M \sqrt{N}. \tag{49}$$

Combining (44) and (49), we arrive at (43) using Theorem 10. ∎

5.6. Nullspace construction via QR decomposition. As in [23], we consider the variant of the QR decomposition $\boldsymbol{B} = \boldsymbol{Q}\boldsymbol{R}$, where the orthogonal transformation of $\boldsymbol{B}$ to upper triangular form is achieved by multiplication by a sequence of M Householder reflectors [17, section 19],

$$\boldsymbol{H}_i = \boldsymbol{I} - 2\boldsymbol{w}_i\boldsymbol{w}_i^{\mathsf{T}}, \quad \boldsymbol{w}_i \in \mathbb{R}^N, \quad \|\boldsymbol{w}_i\|_2 = 1, \quad i = 1, \ldots, M, \tag{50}$$

which introduce zeros below the diagonal in the ith column of $\boldsymbol{B}$ in its successive transformation to the upper triangular $\boldsymbol{R}$. The complete orthogonal transformation is given by $\boldsymbol{Q}^{\mathsf{T}} = \boldsymbol{H}_M \cdots \boldsymbol{H}_1 \in \mathbb{R}^{N\times N}$, and due to the symmetry $\boldsymbol{H}_i = \boldsymbol{H}_i^{\mathsf{T}}$, we have

$$\boldsymbol{D}^{\mathsf{T}}\boldsymbol{A}\boldsymbol{D} = \boldsymbol{Q}^{\mathsf{T}}\boldsymbol{A}\boldsymbol{Q} = \boldsymbol{H}_M \cdots \boldsymbol{H}_1\boldsymbol{A}\boldsymbol{H}_1 \cdots \boldsymbol{H}_M. \tag{51}$$

We can compute $\boldsymbol{Q}^{\mathsf{T}}\boldsymbol{A}\boldsymbol{Q}$ by computing the sequence

$$\boldsymbol{A}_0 = \boldsymbol{A}, \qquad \boldsymbol{A}_i = \boldsymbol{H}_i\boldsymbol{A}_{i-1}\boldsymbol{H}_i, \quad i = 1, \ldots, M, \quad \text{leading to} \quad \boldsymbol{A}_M = \boldsymbol{Q}^{\mathsf{T}}\boldsymbol{A}\boldsymbol{Q}. \tag{52}$$

The transition from $\boldsymbol{A}_{i-1}$ to $\boldsymbol{A}_i$ is a symmetric rank-2 update

$$\begin{aligned} \boldsymbol{A}_i &= (\boldsymbol{I} - 2\boldsymbol{w}_i\boldsymbol{w}_i^{\mathsf{T}})\boldsymbol{A}_{i-1}(\boldsymbol{I} - 2\boldsymbol{w}_i\boldsymbol{w}_i^{\mathsf{T}}) \\ &= \boldsymbol{A}_{i-1} + \begin{pmatrix} \boldsymbol{w}_i & \boldsymbol{A}_{i-1}\boldsymbol{w}_i \end{pmatrix} \begin{pmatrix} 4\boldsymbol{w}_i^{\mathsf{T}}\boldsymbol{A}_{i-1}\boldsymbol{w}_i & -2 \\ -2 & 0 \end{pmatrix} \begin{pmatrix} \boldsymbol{w}_i & \boldsymbol{A}_{i-1}\boldsymbol{w}_i \end{pmatrix}^{\mathsf{T}}. \end{aligned} \tag{53}$$

Based on (53), the sequence (52) can be computed by applying low-rank updates to $\mathcal{H}$-matrices. For implementation purposes, it is most convenient to overwrite $\boldsymbol{A}_{i-1}$ with $\boldsymbol{A}_i$ in (53). This means that the entire sequence (52) can be implemented using only a single $\mathcal{H}$-matrix which is important because the initial $\boldsymbol{A}$ may require a large amount of memory.

An alternative to (53) is to apply each $\boldsymbol{H}_i$ from the left and from the right, separately. However, there are two advantages of applying $\boldsymbol{H}_i$ to both sides of $\boldsymbol{A}_{i-1}$ simultaneously. First, the entire procedure requires only M matrix-vector products $\boldsymbol{A}_{i-1}\boldsymbol{w}_i$ whereas $2M$ individual applications of Householder reflectors $\boldsymbol{H}_i$ would require $2M$ matrix-vector products. Again this is significant if the initial $\boldsymbol{A}$ is large and since the aim of preconditioning is to reduce the number of matrix-vector products in the iterative solution process. Second, the two-sided application of $\boldsymbol{H}_i$ to $\boldsymbol{A}_{i-1}$ means that the entire sequence of $\boldsymbol{A}_i$'s (52) is symmetric whereas the one-sided application of a Householder reflector destroys symmetry. Preserving symmetry ensures that the final result $\boldsymbol{Q}^{\mathsf{T}}\boldsymbol{A}\boldsymbol{Q}$ will be symmetric even in the presence of truncation errors arising from $\mathcal{H}$-arithmetics. It also allows us to only store the upper triangular parts of $\boldsymbol{A}_0, \ldots, \boldsymbol{A}_M$ to save memory.

The fact that the nullspace basis $\boldsymbol{C}$ corresponds to the last $N - M$ columns of the orthonormal matrix $\boldsymbol{Q}$ gives us the following theorem.

THEOREM 12. *The construction of the nullspace basis $\boldsymbol{C}$ via QR factorization results in*

$$\kappa_2(\boldsymbol{C}) = 1, \qquad \kappa_2(\boldsymbol{A}') \le \kappa_2(\widetilde{\boldsymbol{A}}). \tag{54}$$

Proof. The proof follows from Theorem 10. ∎

6. Numerical results. For our numerical tests we implemented Lagrangian augmentation in section 4 and the nullspace method in section 5. For the test problems of relatively small size in section 6.1.1, we use dense matrices and exact arithmetic whereas in all subsequent subsections we replace the main diagonal block by

an $\mathcal{H}$-matrix before applying Lagrangian augmentation or the nullspace method and additional matrix factorizations for preconditioning in $\mathcal{H}$-arithmetic.

This paper does not include numerical results on the error due to the replacement of the main block by an $\mathcal{H}$-matrix since a similar study has already been documented in [19]. In short, the approximation quality of the hybrid RBF interpolant is very similar for both dense and $\mathcal{H}$-matrices when using a high accuracy for the construction of low-rank blocks within the ACA algorithm, in our case $\epsilon_{\mathrm{ACA}} = 10^{-6}$.

The block structure of $\mathcal{H}$-matrices is created by clustering the set of scattered centers X using repeated geometric bisection with a maximum leaf size of $n_{\min} = 40$. For the distinction between low-rank and dense blocks we make use of the standard admissibility condition [14, section 5.4.6] with parameter $\eta = 2$. The computation of $\mathcal{H}$-LU and $\mathcal{H}$-Cholesky factorizations is done with the H2Lib library [5], using respective adaptive accuracies $\epsilon_{\mathrm{LU}} = \epsilon_{\mathrm{Chol}} = 10^{-6}$.

In section 6.1, we investigate the positive definiteness and the condition number of the matrix $\boldsymbol{A}_{\gamma\boldsymbol{W}}$ after Lagrangian augmentation. In addition, we perform tests for the iterative solution of the augmented system using GMRES with $\mathcal{H}$-LU preconditioning.

In section 6.2, we compute the condition number of the projected main block $\boldsymbol{A}' = \boldsymbol{C}^{\mathsf{T}}\boldsymbol{A}\boldsymbol{C}$ of the nullspace method. The linear system $\boldsymbol{A}'\boldsymbol{\alpha}' = \boldsymbol{f}'$ is solved using GMRES preconditioned with an $\mathcal{H}$-Cholesky factorization of $\boldsymbol{A}'$.

All numerical experiments were conducted on a Dell Precision 7810 desktop computer with 32 GB of main memory and two Intel Xeon E5-2690 processors.

6.1. Lagrangian augmentation. In section 6.1.1, we verify that Lagrangian augmentation results in a positive definite matrix $\boldsymbol{A}_{\gamma\boldsymbol{W}}$, provided that γ is chosen as in Theorem 2. For a small number of centers, we compute $\kappa_2(\boldsymbol{A}_{\gamma\boldsymbol{W}})$ and compare it with the bounds from section 4.3.

In section 6.1.2, Lagrangian augmentation is applied for the iterative solution of the interpolation problem using GMRES with both $\mathcal{H}$-LU and no preconditioning.

6.1.1. Positive definiteness. For the numerical experiments in this subsection, we use $N = 2000$ Halton centers [16] in the unit square $[0,1]^2$. The small number of centers allows us to compute the spectrum of the symmetric matrix $\boldsymbol{A}_{\gamma\boldsymbol{W}}$ and to determine $\lambda_{\min}(\boldsymbol{A}_{\gamma\boldsymbol{W}})$ and $\kappa_2(\boldsymbol{A}_{\gamma\boldsymbol{W}})$ using standard array notation and arithmetic for dense matrices without any $\mathcal{H}$-matrix compression. As conditionally positive definite RBFs [27, section 8.4], we consider the multiquadric

$$\phi_{\mathrm{MQ}}(r) = -\sqrt{1+r^2} \quad \text{of order } m = 1 \tag{55}$$

as well as the thin plate spline

$$\phi_{\mathrm{TPS}}(r) = r^2 \log(r) \quad \text{of order } m = 2. \tag{56}$$

The augmented main block $\boldsymbol{A}_{\gamma\boldsymbol{W}} = \boldsymbol{A} + \gamma\boldsymbol{B}\boldsymbol{W}\boldsymbol{B}^{\mathsf{T}}$ is set up in two ways. Either we use $\boldsymbol{W} = \boldsymbol{I}$, resulting in $\boldsymbol{A}_{\gamma\boldsymbol{W}} = \boldsymbol{A} + \gamma\boldsymbol{B}\boldsymbol{B}^{\mathsf{T}}$, or $\boldsymbol{W} = \boldsymbol{R}^{-1}\boldsymbol{R}^{-\mathsf{T}}$, where $\boldsymbol{B} = \boldsymbol{Q}\boldsymbol{R}$ is a QR factorization to produce $\boldsymbol{A}_{\gamma\boldsymbol{W}} = \boldsymbol{A} + \gamma\boldsymbol{Q}\boldsymbol{Q}^{\mathsf{T}}$. Since we want to study the effect of orthonormalizing $\boldsymbol{B}$, we choose $m = 1, 2, 4, 8, 16$ for the polynomial space π^2_m of dimension $M = 1, 3, 10, 36, 136$. The polynomial space is spanned by Legendre polynomials transformed to $[0,1]^2$.

In view of the lower bound (14), the augmentation parameter γ is chosen as

$$\gamma = \begin{cases} \gamma_{\mathrm{ratio}} \, \frac{\|\boldsymbol{A}\|_{\mathrm{F}}}{\sigma_{\min}(\boldsymbol{B})^2} & \text{for} \quad \boldsymbol{W} = \boldsymbol{I}, \\ \gamma_{\mathrm{ratio}} \, \|\boldsymbol{A}\|_{\mathrm{F}} & \text{for} \quad \boldsymbol{W} = \boldsymbol{R}^{-1}\boldsymbol{R}^{-\mathsf{T}}, \end{cases} \tag{57}$$

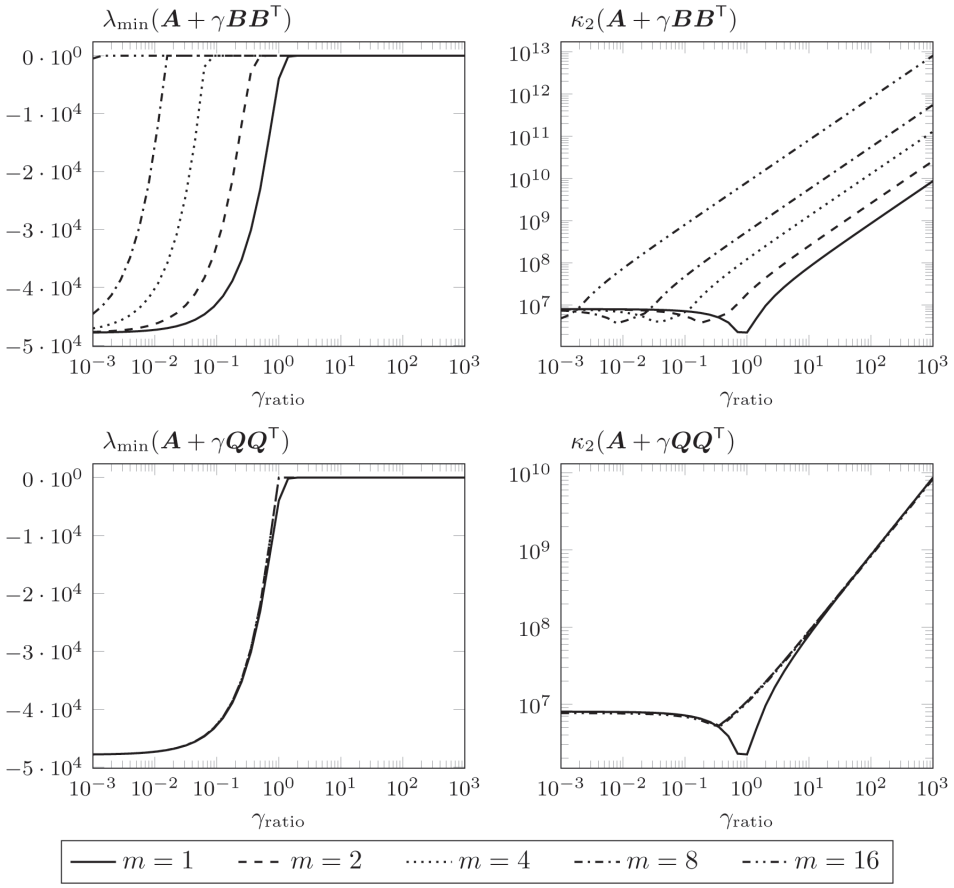

FIG. 3. *Multiquadratics using $N = 2000$ Halton centers in $[0,1]^2$. The smallest eigenvalue and condition number of the main block $\boldsymbol{A}$ after Lagrangian augmentation with $\gamma_{\text{ratio}} \in [10^{-3}, 10^3]$ are shown.*

where the new parameter γ_{ratio} is varied in $[10^{-3}, 10^3]$. In (57), we use $\|\boldsymbol{A}\|_{\text{F}}$ as an upper bound for $\lambda_{\min}(\boldsymbol{A})$ from (14). For larger N, the computation of $\lambda_{\min}(\boldsymbol{A})$ is infeasible whereas $\|\boldsymbol{A}\|_{\text{F}}$ is computable in $\mathcal{O}(N \log N)$ for an $\mathcal{H}$-matrix $\boldsymbol{A}$.

Numerical results for the multiquadric ϕ_{MQ} can be found in Figure 3 where the two plots in the upper row correspond to $\boldsymbol{W} = \boldsymbol{I}$. The plot for $\lambda_{\min}(\boldsymbol{A}+\gamma\boldsymbol{B}\boldsymbol{B}^{\mathsf{T}})$ shows that $\boldsymbol{A}+\gamma\boldsymbol{B}\boldsymbol{B}^{\mathsf{T}}$ becomes positive definite for $\gamma_{\text{ratio}} > 1$ as predicted by Theorem 2. However, we also observe that much smaller values of γ_{ratio} suffice to make $\boldsymbol{A}+\gamma\boldsymbol{B}\boldsymbol{B}^{\mathsf{T}}$ positive definite when $m \neq 1$. The problem with choosing γ_{ratio} larger than necessary can be seen in the plot for $\kappa_2(\boldsymbol{A}+\gamma\boldsymbol{B}\boldsymbol{B}^{\mathsf{T}})$. Once $\lambda_{\min}(\boldsymbol{A}+\gamma\boldsymbol{B}\boldsymbol{B}^{\mathsf{T}})$ is positive, the condition number $\kappa_2(\boldsymbol{A}+\gamma\boldsymbol{B}\boldsymbol{B}^{\mathsf{T}})$ starts to increase together with γ_{ratio} as suggested by the upper bound on $\kappa_2(\boldsymbol{A}_{\gamma\boldsymbol{W}})$ from (25). The effect of orthonormalizing $\boldsymbol{B}$ by choosing $\boldsymbol{W} = \boldsymbol{R}^{-1}\boldsymbol{R}^{-\mathsf{T}}$ can be seen in the bottom pair of plots Figure 3 where for all m the point where $\lambda_{\min}(\boldsymbol{A}+\gamma\boldsymbol{Q}\boldsymbol{Q}^{\mathsf{T}})$ becomes positive is very close to $\gamma_{\text{ratio}} = 1$. Consequently, it is easier to choose γ_{ratio} large enough to make $\boldsymbol{A}+\gamma\boldsymbol{Q}\boldsymbol{Q}^{\mathsf{T}}$ positive definite and avoid an excessive condition number $\kappa_2(\boldsymbol{A}+\gamma\boldsymbol{Q}\boldsymbol{Q}^{\mathsf{T}})$ at the same time.

Similar results as for ϕ_{MQ} are obtained for the thin plate splines ϕ_{TPS}; see Figure 4. Note that for $m = 1$, the matrix $\boldsymbol{A}_{\gamma\boldsymbol{W}}$ remains indefinite for all $\gamma_{\text{ratio}} \in$

$[10^{-3}, 10^3]$ since ϕ_{TPS} is of order $m = 2$.

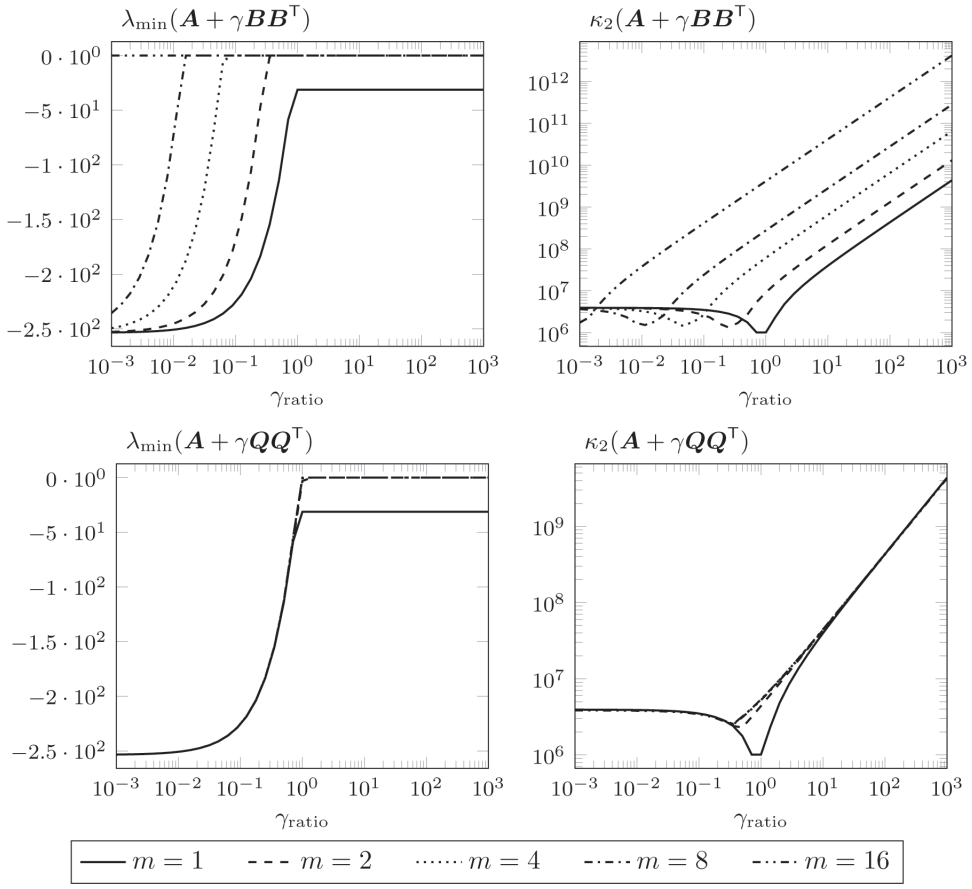

FIG. 4. *Thin plate splines using $N = 2000$ Halton centers in $[0,1]^2$. The smallest eigenvalue and condition number of the main block $\boldsymbol{A}$ after Lagrangian augmentation with $\gamma_{\mathrm{ratio}} \in [10^{-3}, 10^3]$ are shown.*

The condition number of the Schur complement $\boldsymbol{S}_{\gamma \boldsymbol{W}}$ is less important because the size of $\boldsymbol{S}_{\gamma \boldsymbol{W}}$ is small compared to $\boldsymbol{A}_{\gamma \boldsymbol{W}}$. Since the choice $\boldsymbol{W} = \boldsymbol{R}^{-1}\boldsymbol{R}^{-\mathsf{T}}$ was seen to be preferrable to the choice $\boldsymbol{W} = \boldsymbol{I}$, we use only $\boldsymbol{W} = \boldsymbol{R}^{-1}\boldsymbol{R}^{-\mathsf{T}}$ in our plot of $\kappa_2(\boldsymbol{S}_{\gamma \boldsymbol{W}})$ for $\gamma_{\mathrm{ratio}} \in [10^{-3}, 10^3]$ in Figure 5. Once $\gamma_{\mathrm{ratio}} > 1$, the condition number of $\boldsymbol{S}_{\gamma \boldsymbol{W}}$ can be seen to decrease as γ_{ratio} is further increased. This behavior of $\kappa_2(\boldsymbol{S}_{\gamma \boldsymbol{W}})$ seems to be dominated by the decreasing upper bound (28) whereas the increasing upper bound (27) is not visible in Figure 5.

Based on this discussion of the condition numbers of $\boldsymbol{A}_{\gamma \boldsymbol{W}}$ and $\boldsymbol{S}_{\gamma \boldsymbol{W}}$, our recommendation is to choose $\boldsymbol{W} = \boldsymbol{R}^{-1}\boldsymbol{R}^{-\mathsf{T}}$ and γ_{ratio} small but larger than one, e.g., $\gamma_{\mathrm{ratio}} = 2$.

6.1.2. Iterative solution. In our next set of experiments, the Lagrangian augmentation approach is used for the solution of interpolation problems with up to $N = 40000$ quasi-random centers in $[0,1]^2$. Again we use ϕ_{MQ} and ϕ_{TPS} combined with $m \in \{2, 3, 4, 8\}$ for the polynomial space π_m^2.

In the Lagrangian augmentation, we use $\boldsymbol{W} = \boldsymbol{R}^{-1}\boldsymbol{R}^{-\mathsf{T}}$ according to our conclu-

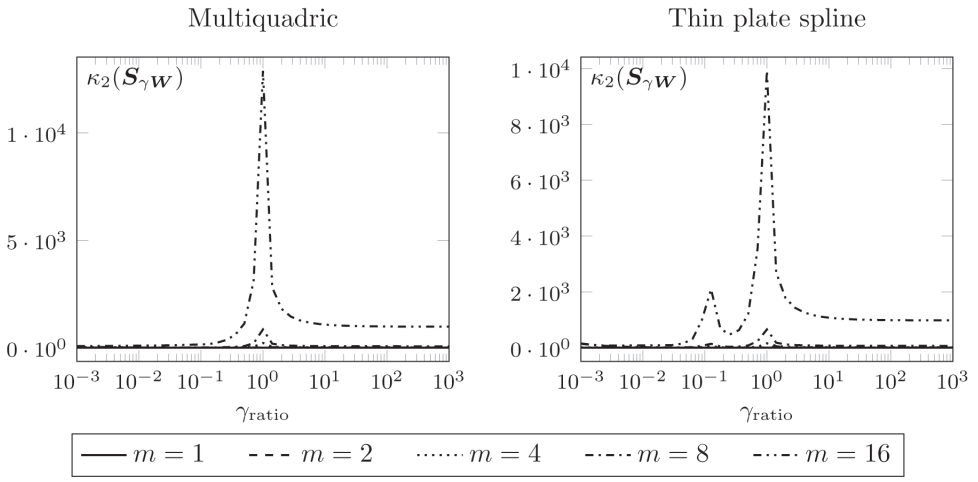

FIG. 5. *Condition number of the Schur complement* $\boldsymbol{S}_{\gamma \boldsymbol{W}}$ *after Lagrangian augmentation with* $\gamma_{\text{ratio}} \in [10^{-3}, 10^3]$ *using* $N = 2000$ *Halton centers in* $[0,1]^2$ *for the multiquadric and thin plate spline RBF.*

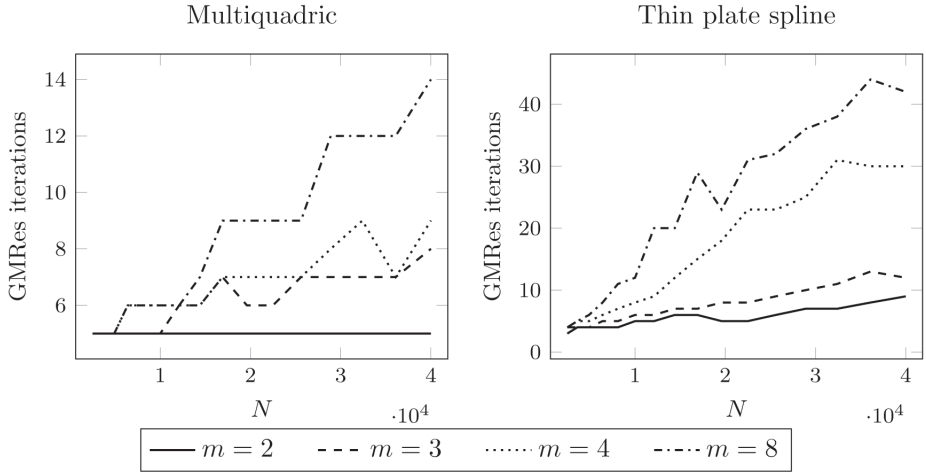

FIG. 6. *Number of GMRES iterations for the solution of an interpolation problem with up to* $N = 40000$ *quasi-random centers in* $[0,1]^2$*, using Lagrangian augmentation combined with an* $\mathcal{H}$*-LU preconditioner.*

sion from the previous section.

After Lagrangian augmentation, the resulting linear system is solved using GMRES preconditioned with an $\mathcal{H}$-LU decomposition of the augmented saddle-point matrix $\widetilde{\boldsymbol{A}}_{\gamma \boldsymbol{W}}$.

In the first set of experiments, we use a fixed parameter $\gamma_{\text{ratio}} = 2$. The number of GMRES iterations required to reduce the norm of the initial residual by a factor of 10^{-6} is shown in Figure 6. For both ϕ_{MQ} and ϕ_{TPS}, the smallest iteration counts are achieved for $m = 2$. For ϕ_{MQ} and $m = 2$, we observe a constant number of five GMRES iterations, independent of N. For ϕ_{TPS} and $m = 2$, the number of iterations

increases slowly with N, up to nine iterations for $N = 40000$.

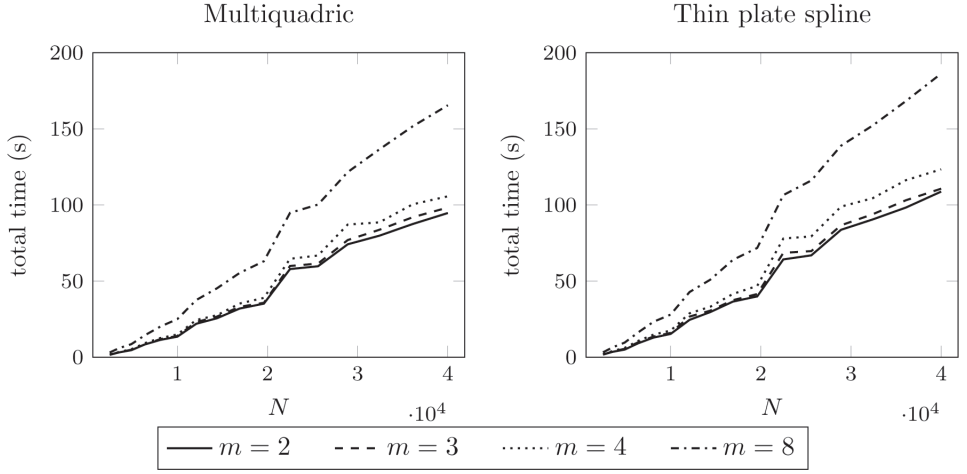

FIG. 7. *Total time for the solution of an interpolation problem with up to $N = 40000$ quasi-random centers in $[0,1]^2$, using Lagrangian augmentation combined with an $\mathcal{H}$-LU preconditioner.*

The time for the solution of the entire interpolation problem is shown in Figure 7. This total solution time includes the construction of $\mathcal{H}$-matrices, the Lagrangian augmentation process, the computation of the $\mathcal{H}$-LU preconditioner, and the subsequent GMRES iterations. In Figure 7, we see that the solution time depends almost linearly on N (for all m). For both RBFs, the total solution time is smallest for $m = 2$, in accordance with our results for the number of iterative solution steps in Figure 6.

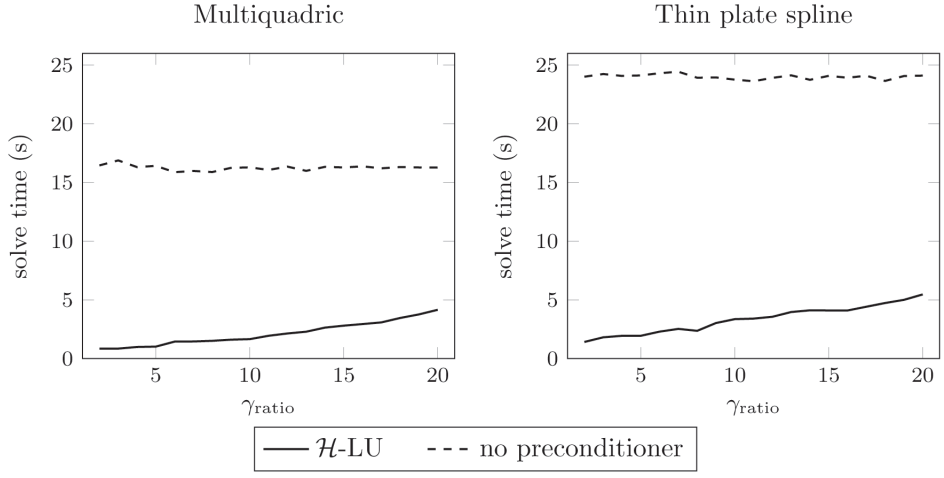

FIG. 8. *GMRES iteration time for an interpolation problem with $N = 40000$ quasi-random centers in $[0,1]^2$ using Lagrangian augmentation with $\gamma_{\text{ratio}} \in \{2, 3, \ldots, 20\}$. The augmented system is solved using either an $\mathcal{H}$-LU or no preconditioner.*

In the following, we compare the iterative GMRES solution of the augmented system using an $\mathcal{H}$-LU preconditioner to using no preconditioner. Here we fix $N =$

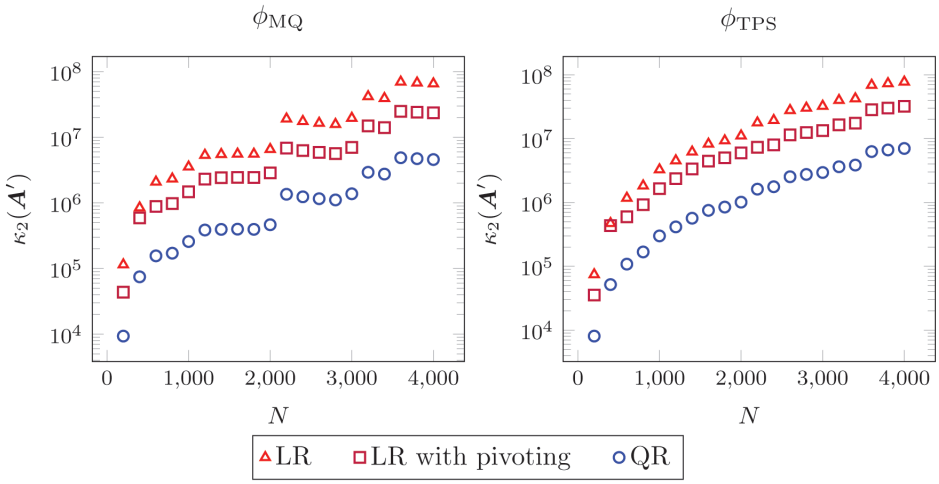

FIG. 9. *Spectral condition number of the projected main block* $\boldsymbol{A}' = \boldsymbol{C}^\mathsf{T}\boldsymbol{A}\boldsymbol{C}$ *depending on the number of Halton centers* $N = 200, \ldots, 4000$ *in* $[0,1]^2$ *using a fixed polynomial order* $m = 2$.

40000 centers and $m = 2$ and vary the augmentation parameter $\gamma_{\mathrm{ratio}} \in \{2, 3, \ldots, 20\}$, keeping in mind that an increase of γ_{ratio} increases the condition number of $\boldsymbol{A}_{\gamma\boldsymbol{W}}$. In Figure 8, we show the time for the GMRES iteration, with qualitatively similar results for both ϕ_{MQ} and ϕ_{TPS}. Using the $\mathcal{H}$-LU preconditioner, we observe a slow increase of the iteration time when γ_{ratio} is increased which might be attributed to the increase in $\kappa_2(\boldsymbol{A}_{\gamma\boldsymbol{W}})$. As expected, without preconditioning the GMRES iteration requires more time than with $\mathcal{H}$-LU preconditioning. However, without preconditioning the iteration time is nearly unaffected by the choice of γ_{ratio}, i.e., a larger $\kappa_2(\boldsymbol{A}_{\gamma\boldsymbol{W}})$ does not lead to higher iteration counts. In order to later compare with timings for the nullspace method, we also provide the total time (here only for $\gamma_{\mathrm{ratio}} = 2$): Using the multiquadric kernel, the total time is 96.8s, which includes the matrix setup and Lagrangian augmentation (3.7s), the $\mathcal{H}$-LU factorization (92.3s), and the GMRES solver (0.8s). For the thin plate spline kernel, the total time is 109.5s, consisting of the matrix setup and Lagrangian augmentation (3.5s), $\mathcal{H}$-LU factorization (104.5s), and GMRES solver (1.4s).

6.2. Nullspace projection. We implemented the projection of the main block $\boldsymbol{A}$ to the nullspace of $\boldsymbol{B}^\mathsf{T}$ in both ways suggested in section 5, i.e., when the nullspace basis $\boldsymbol{C}$ is constructed using either the LU decomposition of section 5.4 or the QR decomposition of section 5.6. In section 6.2.1, we compare the condition numbers of the projected main blocks $\boldsymbol{A}'$.

In section 6.2.2, we illustrate numerical tests where a system involving $\boldsymbol{A}'$ of the nullspace method is solved by an $\mathcal{H}$-Cholesky-preconditioned GMRES iteration.

6.2.1. Conditioning. We use Halton centers in $[0,1]$ to investigate the condition number of the projected main block $\boldsymbol{A}' = \boldsymbol{C}^\mathsf{T}\boldsymbol{A}\boldsymbol{C}$. The computation of $\kappa_2(\boldsymbol{A}')$ requires the setup of $\boldsymbol{A}'$ as a full matrix.

In Figure 9, we compute $\kappa_2(\boldsymbol{A}')$ for a variable number of up to $N = 4000$ centers. Naturally, $\kappa_2(\boldsymbol{A}')$ increases with N for all three nullspace basis variants, with the QR-approach achieving the smallest condition numbers followed by the pivoted and the nonpivoted LU-approaches.

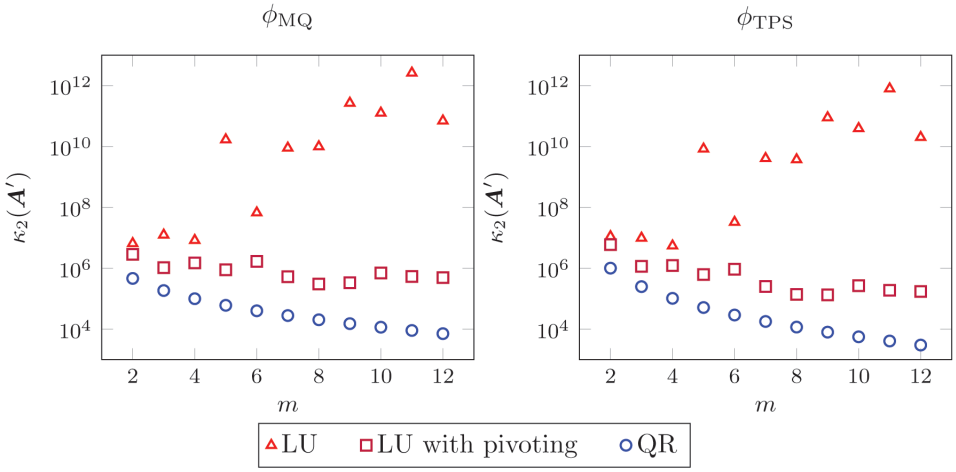

FIG. 10. *Spectral condition number of the projected main block* $\boldsymbol{A}' = \boldsymbol{C}^{\mathsf{T}}\boldsymbol{A}\boldsymbol{C}$ *depending on the polynomial order* $m = 2, \ldots, 12$ *for* $N = 2000$ *Halton centers in* $[0,1]^2$.

In Figure 10, we depict the influence of the polynomial degree on $\kappa_2(\boldsymbol{A}')$ for a fixed number of $N = 2000$ centers. For the nonpivoted LU-approach, $\kappa_2(\boldsymbol{A}')$ increases with m due to ill-conditioning of the nullspace basis. For the pivoted LU-approach, we expected $\kappa_2(\boldsymbol{A}')$ to increase with m as well since the bound (43) is increasing in m. However, in Figure 10, $\kappa_2(\boldsymbol{A}')$ is seen to decrease when m is increased when using the pivoted LU-approach.

An even stronger decrease of $\kappa_2(\boldsymbol{A}')$ is observed for the QR-approach where the nullspace basis $\boldsymbol{C}$ is perfectly conditioned. According to Theorem 10, here the condition number of $\boldsymbol{A}'$ cannot increase, i.e., $\kappa_2(\boldsymbol{A}')$ has to decrease or remain constant. The size of $\boldsymbol{A}' \in \mathbb{R}^{(N-M)\times(N-M)}$ decreases when m is increased, and roughly speaking, for a smaller matrix we would expect a smaller condition number. However, this argument neither explains why $\kappa_2(\boldsymbol{A}')$ is monotonically decreasing for the QR-approach in Figure 10, nor the rate of decay.

6.2.2. Iterative solution. We next compare the effect of the three nullspace basis variants on the iterative solution of the interpolation problem. Once again we set up $\widetilde{\boldsymbol{A}}$ as an $\mathcal{H}$-matrix and transform to block-antitriangular form (32) using $\mathcal{H}$-arithmetics where the low-rank updates in (53) are computed exactly. For the solution of the linear system $\boldsymbol{A}'\boldsymbol{\alpha}' = \boldsymbol{f}'$, we use GMRES with either no preconditioner or an approximate $\mathcal{H}$-Cholesky factorization.

In Figure 11, for $m = 2$ and up to $N = 40000$ quasi-random centers in $[0,1]^2$, we show the total time for the solution of the entire interpolation problem as well as the time needed by the GMRES algorithm to reduce the initial residual by a factor of 10^{-6}. For the QR nullspace basis, the $\mathcal{H}$-Cholesky preconditioned GMRES usually terminates within three iterations. Figure 11 also illustrates that the $\mathcal{H}$-Cholesky preconditioner for the pivoted LU nullspace basis results in moderately larger iteration times compared to the orthogonal basis. For the nonpivoted LU nullspace basis, the $\mathcal{H}$-Cholesky preconditioner performs considerably worse, which we attribute to the ill-conditioning of the nullspace basis.

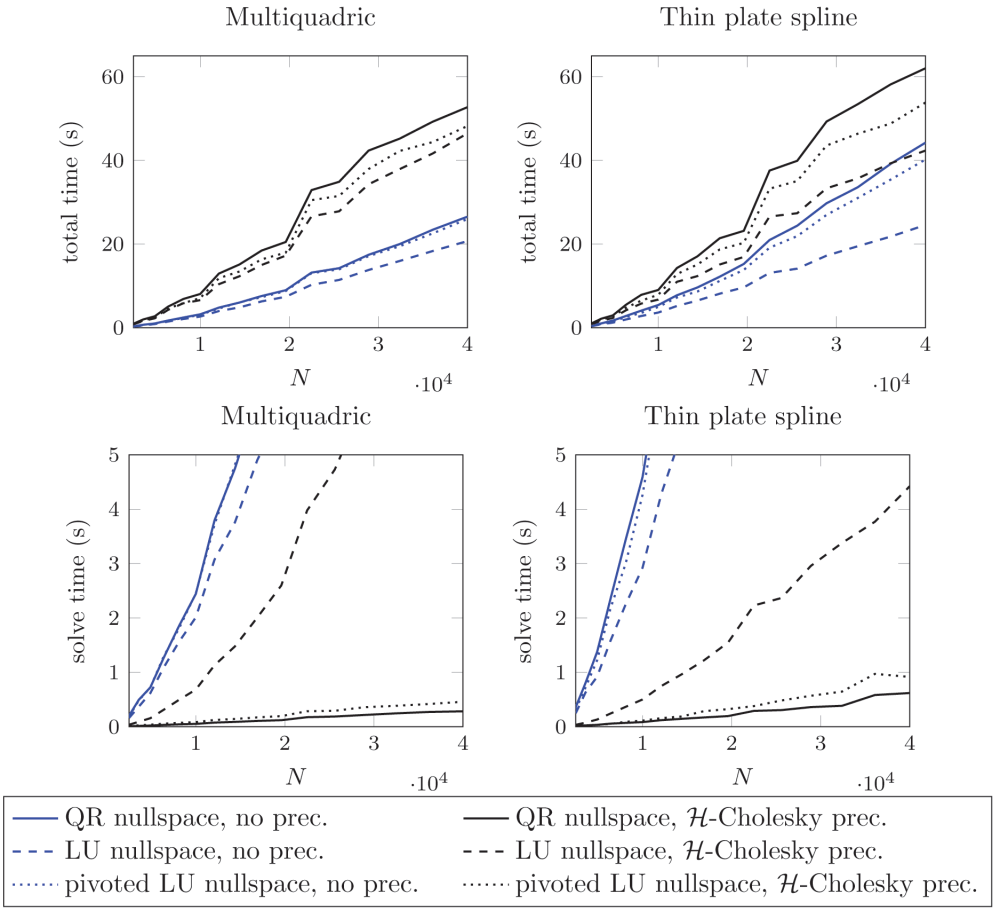

FIG. 11. *Computation times for the solution of an interpolation problem with up to $N = 40000$ quasi-random centers in $[0,1]^2$ using the nullspace method with the three different basis variants. The projected system is solved using either an $\mathcal{H}$-Cholesky or no preconditioner. Both the time for the entire solution of the interpolation problem and the time for the GMRES iteration only are shown.*

Comparing the Lagrangian augmentation to the nullspace approach, we observe that the GMRES iteration times for $N = 40000$ centers are smaller for the nullspace method (in Figure 11) than for the Lagrangian augmentation approach (in Figure 8). In the same way, the total solution time for the nullspace method in Figure 11 is smaller than the total solution time for Lagrangian augmentation method in Figure 7. While the nullspace method has smaller GMRES iteration counts, the major cause for the difference in the total solution times lies in the different constants in the complexity estimates for $\mathcal{H}$-Cholesky and $\mathcal{H}$-LU factorization, the latter having about twice the cost of the former.

7. Conclusions. The focus of this article lies on algebraic preconditioning techniques such as $\mathcal{H}$-Cholesky factorization, applied to scattered data interpolation problems with conditionally positive definite RBFs. While positive definite matrices allow for direct computation of Cholesky factorizations, the indefinite case incorporates new

challenges: it requires a preprocessing step which transforms the indefinite system into a positive definite one. Either Lagrangian augmentation or the nullspace method can be used for such a transformation. We showed that $\mathcal{H}$-matrices are especially convenient to achieve this transformation, since both methods can be formulated in terms of low-rank updates to the original main block $\boldsymbol{A}$. The only requirement for the applicability of the newly proposed methods is that $\boldsymbol{A}$ is positive definite on $\ker(\boldsymbol{B}^{\mathsf{T}})$.

For the implementation of the nullspace method within the framework of $\mathcal{H}$-matrices, it was useful to interpret the nullspace method as an antitriangular factorization of $\widetilde{\boldsymbol{A}}$ as in [21, 22]. Computing the antitriangular factorization of $\mathcal{H}$-matrices allowed us to implement the nullspace method using either a sparse or an orthogonal basis in a uniform way.

For the Lagrangian augmentation approach, we provide a lower bound γ_0 for the augmentation parameter to guarantee positive definiteness of the augmented matrix as well as upper bounds for the condition number of the transformed matrix. While these bounds are not sharp, they suggest an increase in condition number when the augmentation parameter γ is further increased beyond γ_0, which is actually observed in the numerical tests and coupled with an increase in iterative solution times for the preconditioned GMRES solver.

We also prove bounds for the condition number of the projected block A' in the nullspace method depending on the type of nullspace basis construction. Once again these bounds are not sharp, but they are supported by numerical results: The orthogonal nullspace basis led to a smaller condition number of the projected main block $\boldsymbol{A'}$ (30) and fewer iterative steps in the subsequent solution of the preconditioned linear system compared to the sparse, LU-based nullspace basis.

For $N \geq 40000$ centers, both Lagrangian augmentation and the nullspace method, followed by an iterative solution with $\mathcal{H}$-Cholesky preconditioning, become less effective (with the nullspace method appearing to be more robust than Lagrangian augmentation).

This is because the time to compute the $\mathcal{H}$-Cholesky factorization gets undesirably large and the number of iterative solution steps increases when the number of centers N is further increased. More severely, for large N, the factorization process is susceptible to break-downs, i.e., the factorization may not complete in the first place.

A remedy to such a breakdown is offered in [2], however, for even increased computational cost and without significantly reducing the number of required iterative steps. The latter would require a higher $\mathcal{H}$-accuracy for which, in turn, the standard $\mathcal{H}$-Cholesky factorization might be computable without any breakdown.

Hence, $\mathcal{H}$-matrix techniques certainly lead to (storage and computational) savings in the construction of the interpolation matrices as well as the Lagrangian augmentation and nullspace preprocessing proposed in this paper. For the subsequent construction of a (factorization based) preconditioner, they currently appear to be rather expensive (even though of almost optimal complexity). However, comparing our numerical results obtained for preconditioned and unpreconditioned iterative solvers motivates the search for less expensive preconditioners (e.g., outside the $\mathcal{H}$-matrix framework).

In addition, while not practical as stand-alone solvers for $N \geq 40000$ centers, the techniques of this paper are well suited as subdomain solvers in domain decomposition approaches for even larger numbers of centers, a topic which we have pursued in [8].

REFERENCES

[1] R. K. Beatson, W. A. Light, and S. Billings, *Fast solution of the radial basis function interpolation equations: Domain decomposition methods*, SIAM J. Sci. Comput., 22 (2001), pp. 1717–1740, https://doi.org/10.1137/S1064827599361771.

[2] M. Bebendorf and W. Hackbusch, *Stabilized rounded addition of hierarchical matrices*, Numer. Linear Algebra Appl., 14 (2007), pp. 407–423.

[3] M. Benzi, G. H. Golub, and J. Liesen, *Numerical solution of saddle point problems*, Acta Numer., 14 (2005), pp. 1–137, https://doi.org/10.1017/S0962492904000212.

[4] M. Benzi and M. A. Olshanskii, *An augmented Lagrangian-based approach to the Oseen problem*, SIAM J. Sci. Comput., 28 (2006), pp. 2095–2113, https://doi.org/10.1137/050646421.

[5] S. Börm, *H2LIB Software Library*, University of Kiel, Kiel, Germany, http://www.h2lib.org, 2017.

[6] S. Börm and S. Le Borne, *$\mathcal{H}$-LU factorization in preconditioners for augmented Lagrangian and grad-div stabilized saddle point systems*, Internat. J. Numer. Methods Fluids, 68 (2012), pp. 83–98, https://doi.org/10.1002/fld.2495.

[7] S. Le Borne, *Block computation and representation of a sparse nullspace basis of a rectangular matrix*, Linear Algebra Appl., 428 (2008), pp. 2455–2467, https://doi.org/10.1016/j.laa.2007.11.025.

[8] S. Le Borne and M. Wende, *Domain decomposition methods in scattered data interpolation with conditionally positive definite radial basis functions*, Comput. Math. Appl. 77 (2019), pp. 1178–1196, https://doi.org/10.1016/j.camwa.2018.10.042.

[9] S. Boyd and L. Vanderberghe, *Convex Optimization*, 7th printing with corrections, Cambridge University Press, Cambridge, UK, 2009.

[10] F. Cheng, *On conditioning of saddle-point matrices with Lagrangian augmentation*, Appl. Math. Comput., 248 (2014), pp. 4–7.

[11] J. Cherrie, R. Beatson, and G. Newsam, *Fast evaluation of radial basis functions: Methods for generalized multiquadrics in $\mathbb{R}^n$*, SIAM J. Sci. Comput., 23 (2002), pp. 1549–1571, https://doi.org/10.1137/S1064827500367609.

[12] M. Fortin and R. Glowinski, *Augmented Lagrangian Methods: Applications to the Numerical Solution of Boundary-Value Problems*, Stud. Math. Appl. 15, North-Holland, Amsterdam, 1983.

[13] G. H. Golub and C. Greif, *On solving block-structured indefinite linear systems*, SIAM J. Sci. Comput., 24 (2003), pp. 2076–2092, https://doi.org/10.1137/S1064827500375096.

[14] W. Hackbusch, *Hierarchical Matrices: Algorithms and Analysis*, Springer Ser. Comput. Math. 49, Springer, Heidelberg, 2015, https://ebookcentral.proquest.com/lib/gbv/detail.action?docID=4213051.

[15] W. Hackbusch, *Iterative Solution of Large Sparse Systems of Equations*, 2nd ed., Springer, Cham, 2016, https://doi.org/10.1007/978-3-319-28483-5.

[16] J. Halton, *On the efficiency of certain quasi-random sequences of points in evaluating multi-dimensional integrals*, Numer. Math., 2 (1960), pp. 84–90, https://doi.org/10.1007/BF01386213.

[17] N. J. Higham, *Accuracy and Stability of Numerical Algorithms*, SIAM, Philadelphia, 2002, https://doi.org/10.1137/1.9780898718027.

[18] N. J. Higham, *A survey of condition number estimation for triangular matrices*, SIAM Rev., 29 (1987), pp. 575–596, https://doi.org/10.1137/1029112.

[19] A. Iske, S. Le Borne, and M. Wende, *Hierarchical matrix approximation for kernel-based scattered data interpolation*, SIAM J. Sci. Comput., 39 (2017), pp. A2287–A2316, https://doi.org/10.1137/16M1101167.

[20] Q. T. Le Gia, I. H. Sloan, and A. J. Wathen, *Stability and preconditioning for a hybrid approximation on the sphere*, Numer. Math., 118 (2011), pp. 695–711, https://doi.org/10.1007/s00211-011-0369-0.

[21] N. Mastronardi and P. Van Dooren, *The antitriangular factorization of symmetric matrices*, SIAM J. Matrix Anal. Appl., 34 (2013), pp. 173–196, https://doi.org/10.1137/110858860.

[22] J. Pestana and A. J. Wathen, *The antitriangular factorization of saddle point matrices*, SIAM J. Matrix Anal. Appl., 35 (2014), pp. 339–353, https://doi.org/10.1137/130934933.

[23] M. Powell, *Some algorithms for thin plate spline interpolation to functions of two variables*, in Proceedings of the Conference on Advances in Computational Mathematics, World Scientific, River Edge, NJ, 1994, pp. 303–319.

[24] T. Rees and J. Scott, *A comparative study of null-space factorizations for sparse symmetric saddle point systems*, Numer. Linear Algebra Appl., 25 (2018), e2103, https://doi.org/10.1002/nla.2103.

[25] G. Roussos and B. J. Baxter, *Rapid evaluation of radial basis functions*, J. Comput. Appl. Math., 180 (2005), pp. 51–70, https://doi.org/10.1016/j.cam.2004.10.002.

[26] Y. Saad, *Iterative Methods for Sparse Linear Systems*, 2nd ed., SIAM, Philadelphia, 2003, https://doi.org/10.1137/1.9780898718003.

[27] H. Wendland, *Scattered Data Approximation*, Cambridge Monogr. Appl. Comput. Math. 17, Cambridge University Press, Cambridge, UK, 2010.

[28] R. Yokota, L. A. Barba, and M. G. Knepley, *PetRBF—a parallel $\mathcal{O}(N)$ algorithm for radial basis function interpolation with Gaussians*, Comput. Methods Appl. Mech. Engrg., 199 (2010), pp. 1793–1804.